medRxiv preprint doi: https://doi.org/10.1101/2020.01.20.20018069; this version posted January 27, 2020. The copyright holder has placed this preprint (which was not certified by peer review) in the Public Domain. It is no longer restricted by copyright. Anyone can legally share, reuse, remix, or adapt this material for any purpose without crediting the original authors.

Early signs of disrupted rule learning in adolescents at clinical high risk for psychosis

Joseph M. Orr[1,2], Jesus Lopez[1], Michael J. Imburgio[1], Andrea Pelletier-Baldeli[3], Jessica A. Bernard[1,2], & Vijay A. Mittal[4,5,6,7]

[1] Department of Psychological and Brain Sciences,
[2] Texas A&M Institute for Preclinical Studies
Texas A&M University
College Station, Texas

[3]Department of Psychiatry,
UNC-Chapel Hill School of Medicine
Chapel Hill, North Carolina

[4] Department of Psychiatry,
[5] Medical Social Sciences,
[6] Institute for Policy Research (IPR),
[7] Institute for Innovations in Developmental Sciences (DevSci)
Northwestern University
Evanston, Illinois

Address correspondence to:
Joseph M. Orr, Ph.D.
515 Coke Street
4235 TAMU
College Station, TX 77843-4235
Email: joseph.orr@tamu.edu
Phone: (979)845-6368

Keywords: high risk, psychosis, fMRI, executive function, rule learning, imaging

NOTE: This preprint reports new research that has not been certified by peer review and should not be used to guide clinical practice.

medRxiv preprint doi: https://doi.org/10.1101/2020.01.20.20018069; this version posted January 27, 2020. The copyright holder has placed this preprint (which was not certified by peer review) in the Public Domain. It is no longer restricted by copyright. Anyone can legally share, reuse, remix, or adapt this material for any purpose without crediting the original authors.

Abstract

Background: The ability to flexibly apply rules to novel situations is a critical aspect of adaptive human behavior. Evidence from traditional neuropsychological tests suggest that broad executive function deficits appear early in the course of psychosis, but it is unclear which specific facets are affected. Identifying whether rule learning is impacted at the early stages of psychosis are necessary for truly understanding the etiology of psychosis and may be critical for designing novel treatments. Therefore, we examined rule learning in healthy adolescents and those meeting criteria for clinical high risk (CHR) for psychosis.

Methods: 24 control and 22 CHR adolescents underwent rapid, high-resolution fMRI while performing a paradigm which required them to apply novel or practiced task rules.

Results: Previous work with this task has suggested that practiced rules rely on rostrolateral prefrontal cortex (RLPFC) during task preparation and dorsolateral prefrontal cortex (DLPFC) during task performance, while novel rules showed the opposite pattern. In controls, we partially replicated this finding with a small effect of greater activity in RLPFC for practiced versus novel tasks; however, the CHR group showed a dysfunctional pattern of results. Not only did the CHR group show alternations in the expected brain dynamics, but they showed weaker effects than controls during both task preparation and task performance.

Conclusions: These findings suggest that the critical ability to flexibly apply abstract rules is already disrupted at the clinical high risk stage of psychosis. However, more data is needed to determine whether these deficits predict disease progression.

medRxiv preprint doi: https://doi.org/10.1101/2020.01.20.20018069; this version posted January 27, 2020. The copyright holder has placed this preprint (which was not certified by peer review) in the Public Domain. It is no longer restricted by copyright. Anyone can legally share, reuse, remix, or adapt this material for any purpose without crediting the original authors.

Introduction

Unlike most laboratory animals that require extensive training to acquire a task, humans have the ability to rapidly acquire new tasks based on limited instructions. This ability, a critical component of the broader construct of executive function, is critical in dynamic environments where one must adapt practiced knowledge to new instructions (Braver and Barch, 2006; Monsell, 1996; Woolgar et al., 2011). It is generally accepted that these executive function processes are coordinated by the frontal lobes (Duncan, 2010, 1986; 2001; Stuss and Alexander, 2000). Dysfunction of the frontal lobes has been widely described in schizophrenia, from studies of task-related functional activation (MacDonald and Carter, 2003; Minzenberg et al., 2009; Poppe et al., 2016), resting-state functional connectivity (Pettersson-Yeo et al., 2011; Repovs et al., 2011; Rotarska-Jagiela et al., 2010; Zhou et al., 2007), white matter connectivity (Camchong et al., 2009; Oh et al., 2009; van den Heuvel et al., 2010), and structural morphometry (Gur et al., 2000; Sallet et al., 2003). Moreover, it has been suggested that dysfunction of the dorsolateral prefrontal cortex (DLPFC) is related to deficits in the ability to maintain task rules and goals, a core deficit of schizophrenia. Increasing evidence suggests that executive function deficits and prefrontal dysfunctions are present at the prodromal or risk stage of schizophrenia (Allen et al., 2012; Fornito et al., 2013; Fusar-Poli et al., 2011; Harris et al., 2004; Morey et al., 2005; Seidman et al., 2006; Stanfield et al., 2008).

The onset of psychosis is usually preceded by a prodromal phase characterized by functional decline and subtle attenuated symptoms that include positive phenomena and a decline in socio-occupational functioning (Yung and McGorry, 1996). Those at clinical high-risk (CHR; i.e, meeting criteria for a psychosis risk syndrome) are of critical importance as the prodromal period is

medRxiv preprint doi: https://doi.org/10.1101/2020.01.20.20018069; this version posted January 27, 2020. The copyright holder has placed this preprint (which was not certified by peer review) in the Public Domain. It is no longer restricted by copyright. Anyone can legally share, reuse, remix, or adapt this material for any purpose without crediting the original authors.

of interest both as a window for investigating processes involved in disease onset, and also as a potential point of intervention and prevention (Haroun et al., 2006; McGlashan et al., 2007; Thompson et al., 2015). More specifically, recent studies have suggested that adolescents with a prodromal syndrome (i.e., showing moderate attenuated positive symptoms accompanied by a global decline in functioning) (Miller et al., 1999; Woods et al., 2014) are at imminent risk for conversion to a psychotic disorder; although successful early identification and other factors relating to heterogeneous assessment/inclusion criteria have yielded a global decrease in transition rates (Fusar-Poli et al., 2016; Yung et al., 2007), a substantial proportion (anywhere from 10-35%) will convert to a psychotic disorder within a two-year period (Cannon et al., 2016, 2008; Yung et al., 2007). This is promising from a research perspective as prospective understanding of brain structure and function, in the period prior to when medications and neurotoxicity can confound research, is likely to significantly inform etiological conceptualizations of psychosis (Damme et al., 2019a; P. Fusar-Poli et al., 2012; Haroun et al., 2006). It is also significant from a clinical perspective as better understanding of the high-risk period will help to implement early intervention and guide treatment decisions with the potential to reduce the duration of untreated psychosis (White et al., 2006), ameliorate course of illness, and delay or potentially prevent the onset of psychosis (McGlashan et al., 2001). Because schizophrenia severely limits the most productive years of an individual's life its costs to society are enormous (Cloutier et al., 2016), and this promise of early detection and intervention represents a major breakthrough.

While existing cognitive-behavioral (Morrison et al., 2012, 2004), psychopharmacological (McGlashan et al., 2003; Woods et al., 2013, 2007), and supplemental treatments (Amminger et al., 2010) have shown noteworthy effects, to date there have been no conclusive empirically supported

medRxiv preprint doi: https://doi.org/10.1101/2020.01.20.20018069; this version posted January 27, 2020. The copyright holder has placed this preprint (which was not certified by peer review) in the Public Domain. It is no longer restricted by copyright. Anyone can legally share, reuse, remix, or adapt this material for any purpose without crediting the original authors.

interventions for CHR youth (Corcoran et al., 2010; Preti and Cella, 2010). Furthermore, there are significant treatment costs associated with psychotherapy, and serious adverse side effects accompanying pharmacological intervention (e.g. weight gain, related diabetes). There is a critical need for innovative new treatment options. Recent cognitive remediation trials in psychosis have demonstrated benefits from neuroplasticity based interventions and that intensive trials engaging effortful activity are feasible in CHR samples (Fisher et al., 2013; Holzer et al., 2014; Hooker et al., 2014). As impairments in executive function may be an important marker of whether an individual is at risk for psychosis (Niendam et al., 2014), early interventions should target executive functioning. However, a review of cognitive intervention in early psychosis suggested that targeting cognitive domains that are impaired early in the course of psychosis, like executive function, is not as effective as interventions that seek to sustain intact abilities (Pantelis et al., 2015). Nevertheless, most cognitive interventions have been designed to target broad aspects of executive, not specific facets such as rule learning or goal maintenance; therefore, gaining a detailed understanding of the specific executive function deficits is critical towards developing an etiology of psychosis.

While cognitive impairments have been well documented in psychosis risk, including in broad domains of executive function (Bora and Murray, 2014; Carrión et al., 2018; Paolo Fusar-Poli et al., 2012), these deficits have largely been demonstrated with traditional neuropsychological assessments. This makes it difficult to determine what specific executive function deficits are present in the high-risk period of psychosis. Recently, Guo and colleagues (Guo et al., 2019) examined whether performance on the AX-CPT—a task thought to measure context or goal maintenance—predicted progression (i.e., conversion risk) in an at-risk population. They found that baseline performance on the AX-CPT was predictive of clinical status 12 months later. This study

medRxiv preprint doi: https://doi.org/10.1101/2020.01.20.20018069; this version posted January 27, 2020. The copyright holder has placed this preprint (which was not certified by peer review) in the Public Domain. It is no longer restricted by copyright. Anyone can legally share, reuse, remix, or adapt this material for any purpose without crediting the original authors.

confirms earlier proposals of context/goal maintenance as a marker of psychosis risk (Niendam et al., 2014), and is in line with the suggestion that goal maintenance is a core deficit of schizophrenia (Barch and Ceaser, 2012).

While adaptive executive function has been extensively studied in behavioral and neuroimaging studies, these studies have largely relied on highly practiced tasks. Dumontheil and colleagues (2011) demonstrated that new rules are encoded across a broad network of frontal and parietal regions that Duncan (2010) has referred to as the Multiple Demand Network. As tasks become more difficult (but not necessarily more abstract or complex), more rostral regions of the frontal lobes come online (2012). However, several studies on rapid instructed task learning (RITL) by Cole and colleagues (2017, 2016, 2010) have shown that practiced and novel tasks rely on the same regions of the lateral frontal cortex, but the temporal dynamics of these regions varies based on novelty. They demonstrated that practiced task rule encoding relies on the rostrolateral prefrontal cortex (RLPFC) for retrieving task rules from long-term memory, and subsequent rule activation by the dorsolateral prefrontal cortex (DLPFC) for task performance. Novel task preparation showed a reversal of these dynamics, such that the novel rules are encoding in a bottom-up fashion by the DLPFC and become integrated by the RLPFC during task performance. However, there have been no investigations of whether psychosis risk is associated with deficits in learning new rules/tasks

In order to better understand which executive function processes are impaired among those at high-risk for psychosis, and map the affected underlying neurobiology, we investigated RITL in CHR adolescents and healthy controls (HC). The paradigm was adapted from the Permuted Rule Operations task of Cole and colleagues (2010), with timing modified slightly for fast multiband fMRI. Participants were extensively trained on 4 combinations of rules about a week before

medRxiv preprint doi: https://doi.org/10.1101/2020.01.20.20018069; this version posted January 27, 2020. The copyright holder has placed this preprint (which was not certified by peer review) in the Public Domain. It is no longer restricted by copyright. Anyone can legally share, reuse, remix, or adapt this material for any purpose without crediting the original authors.

scanning. During scanning, participants saw these same 4 practiced rules, as well 60 novel rule combinations. Given the evidence discussed above that goal maintenance, supported by activity in the DLPFC, is impacted across the psychosis spectrum (MacDonald et al., 2005; Niendam et al., 2014; Poppe et al., 2016), we predicted that CHR participants would show decreased DLPFC activation during novel task rule encoding. Furthermore, in line with the idea that the DLPFC is critical for task rule encoding, we predicted that practiced tasks would be associated with decreased RLPFC activation during encoding and decreased DLPFC activation during performance. Within control participants, we expected to replicate the DLPFC-RLPFC dynamics previously demonstrated by Cole and colleagues (2010).

Methods

Participants

Here, we investigated 23 adolescent and young adult CHR participants (mean age= 20.8 + 1.54 years, 7 female), and 25 HC participants (mean age = 21.5 + 1.83 years, 11 female). All participants had previously enrolled in a longitudinal study investigating psychosis risk as part of the Adolescent Development and Preventative Treatment (ADAPT) research program at the University of Colorado Boulder. Participants were recruited for participation in this investigation at the end of their annual study visit, or were directly contacted over the phone. In addition to the current procedures, participants also completed 2 other short paradigms in the same scanning session (Damme et al., 2019b; Pelletier-Baldelli et al., 2018). Prior to participating in the imaging study, all participants were consented specifically for the imaging study, and declining to participate did not affect their participation in the ongoing longitudinal study. All procedures were reviewed and approved by the University of Colorado Boulder Institutional Review Board.

medRxiv preprint doi: https://doi.org/10.1101/2020.01.20.20018069; this version posted January 27, 2020. The copyright holder has placed this preprint (which was not certified by peer review) in the Public Domain. It is no longer restricted by copyright. Anyone can legally share, reuse, remix, or adapt this material for any purpose without crediting the original authors.

Exclusion criteria for both groups included a history of head injury, the presence of a neurological disorder, life-time substance dependence as assessed by the Structured Clinical Interview for Axis-I DSM IV Disorders (First et al., 1995), and the presence of any contraindications for the magnetic resonance imaging environment. In the CHR group, we also excluded individuals with an Axis I psychotic disorder. In the control sample, we excluded individuals with any diagnosis of an Axis I disorder. Further, the presence of a psychotic disorder in first-degree relatives was an additional exclusion criterion for the control group. Due to response box errors (1 CHR participant) and a failure to follow task instructions (1 HC participant), the final sample included 46 participants. See Table 1 for demographics and symptom information.

Symptom Assessment

The Structured Interview for Prodromal Syndromes (SIPS) measures distinct categories of prodromal symptom domains (positive, negative, disorganized, general) and is scored from 0-6 for each symptom. Inclusion in the CHR group was determined by moderate levels of positive symptoms (a SIPS score of 3-5 in one or more of the 5 positive symptom categories), and/or a decline in global functioning in association with the presence of schizotypal personality disorder, and/or a family history of schizophrenia (Miller et al., 1999). All interviewers had inter-rater reliabilities that exceeded Kappa $\geq$ 80. We confirmed CHR diagnosis for those who participated more than 1 month from entry to larger CHR study protocols. All CHR participants were not taking antipsychotics at the time of participation.

Permuted Rule Operations (PRO) Paradigm

The Permuted Rule Operations (PRO) Paradigm was adapted from E-Prime code kindly provided by Michael W. Cole and is described in full detail elsewhere (Cole et al., 2010). This

medRxiv preprint doi: https://doi.org/10.1101/2020.01.20.20018069; this version posted January 27, 2020. The copyright holder has placed this preprint (which was not certified by peer review) in the Public Domain. It is no longer restricted by copyright. Anyone can legally share, reuse, remix, or adapt this material for any purpose without crediting the original authors.

paradigm combines 3 types of cues (logic cue, semantic cue, and response cue), each with 4 possibilities to yield 64 possible rule- or task-sets that describe how the participant was to respond to a set of 3 pairs of trial stimuli (See Figure 1). The trial stimuli consisted of concrete nouns and a participant's task was to indicate whether the stimuli were True or False with respect to the rule. The response cue indicated which button was to be used to indicate True, and the other possible finger (index or middle) of the same hand was to be used to indicate False. The same rule applied to all three trials in a block. For example, if the set of cues was SAME (logic cue), SWEET (semantic cue), and LEFT INDEX (response cue), and the trial stimuli were SEAWEED + TURNIP, GRAPE + APPLE, and FUR + SUGAR, a participant would respond TRUE (both are not sweet), TRUE (both are not sweet), FALSE (one is not sweet, the other is sweet). At the beginning of an experimental block the cues were presented one at a time, each for 0.92s (2 TR). After a variable delay between 1.84s and 5.98s (4-6 TR), participants performed 3 trials. On each trial, the two stimuli were presented one at a time, each for 0.92s (2 TR); participants were instructed to respond after the second stimuli was presented. There was a variable inter-trial delay between 1.84s and 5.98s (4-12 TR), and a variable inter-block interval between 11.96s and 16.1s (24-36 TR).

Of these 64 possible rules, 4 were randomly selected to be practiced during a pre-scan training session which occurred about a week prior to the scan; the practiced rules were counterbalanced across participants. During training, participants received extensive instruction on how to apply the rules, with self-paced examples. Once they understood the instructions, participants completed 12 runs of training, each consisting of 12 blocks of trials with each of the 4 rules being presented 3 times. The first 2 runs were self-paced practice with feedback. After practice, they completed 10 runs without feedback with the same timing as the scanner. They were given time

medRxiv preprint doi: https://doi.org/10.1101/2020.01.20.20018069; this version posted January 27, 2020. The copyright holder has placed this preprint (which was not certified by peer review) in the Public Domain. It is no longer restricted by copyright. Anyone can legally share, reuse, remix, or adapt this material for any purpose without crediting the original authors.

to rest in between blocks. During scanning, participants performed 6 runs consisting of 6 novel and 6 practiced rule blocks. Each novel rule was only presented once in a session, so that not all 64 rules were seen by all participants.

Behavioral data from the training session and the scanning session were analyzed using *jamovi (v. 1.0, The jamovi project, 2019)*, a free software package that runs on R. Only correct reaction times were analyzed, and reaction time data and accuracy data were checked for violations of normality with Shapiro-Wilk tests. When normality was violated, non-parametric tests were used.

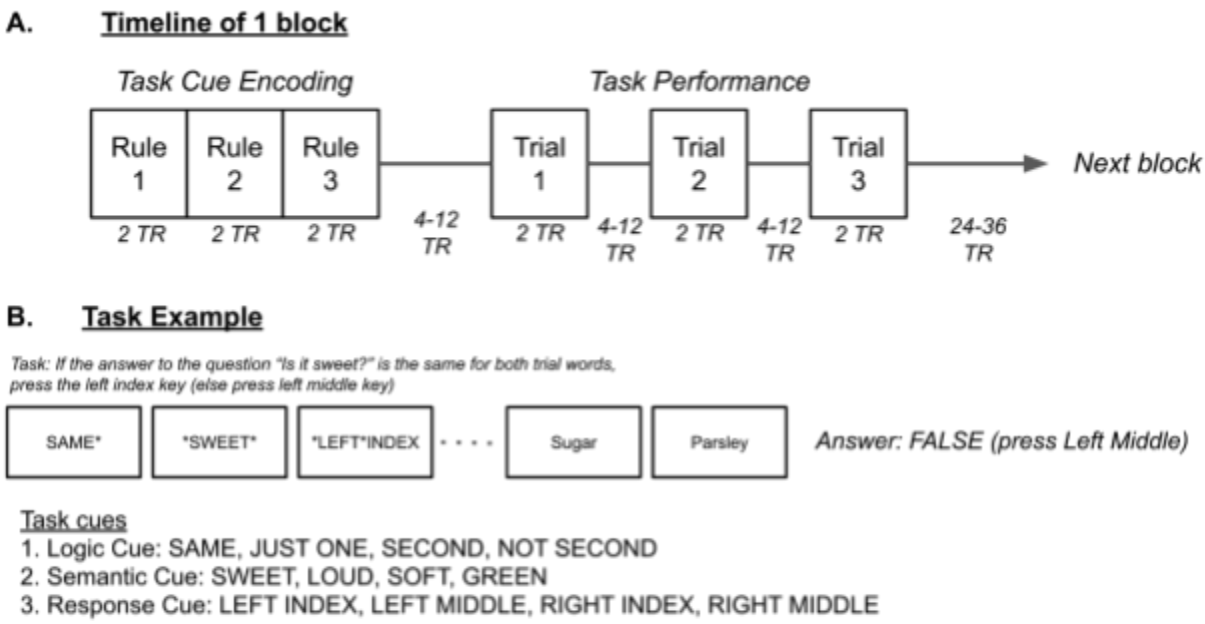

Figure 1. A. Example task block. At the beginning of a block three instruction cues were presented that defined the current task. Each cue was presented one at a time in the following order: logic cue, semantic cue, response cue. There were 4 possible logic cues, 4 possible semantic cues, and 4 possible response cues, yielding 64 possible tasks from all combinations. Of the 64 possible tasks, 4 were practiced before scanning and the remainder were only shown once each in a scanning session. Participants then performed three trials of the task, indicating if the current task rule was true or false. B. Example of one possible task formed by the combination (SWEET* SAME* *LEFT *INDEX), instructing the participant to judge whether or not both of the trial words are sweet and respond true with the left index key.

Data Sharing

Behavioral data and analysis scripts are available on Open Science Framework (https://osf.io/snuqj/). Raw imaging data is available on OpenNeuro

medRxiv preprint doi: https://doi.org/10.1101/2020.01.20.20018069; this version posted January 27, 2020. The copyright holder has placed this preprint (which was not certified by peer review) in the Public Domain. It is no longer restricted by copyright. Anyone can legally share, reuse, remix, or adapt this material for any purpose without crediting the original authors.

(doi://10.18112/openneuro.ds001371.v1.0.0). Final statistical results are available on BALSA (to be uploaded when figures are finalized). Additional information about symptoms and demographics are not publicaly available, but can be made available by contacting author VAM.

fMRI Data Acquisition

All functional imaging data was collected using a 3T Siemens Magnetom Tim Trio (software version VB17A; Munich, Germany), using multi-band functional pulse sequences with a 32-channel head coil. Sequences for multi-band functional imaging were acquired from the Center for Magnetic Resonance Research (http://www.cmrr.umn.edu/multiband/index.shtml) and modified as needed for the UCB scanner. Structural images were acquired using a sagittal T1-weighted interleaved sequence (repetition time (TR) = 2400 ms, echo-time (TE) = 2.01 ms, echo spacing = 7.4 ms, flip angle = 8°, field-of-view = 256 mm x 256 mm x 180 mm, voxel resolution = 0.8 mm isotropic). Six runs of multiband EPIs were acquired in the posterior to anterior direction with the following parameters (multiband acceleration factor = 8, bandwidth = 2772 Hz/Px, TR = 460 ms, TE = 29.0, echo-spacing = 0.51 ms, flip-angle = 44°, field-of-view = 248 x 248 x 168 mm, voxel resolution = 3.0 mm isotropic, number of slices = 56, time = 4:00 minutes). We also collected two brief (2 volumes each) scans prior to each of the functional imaging runs, using the same EPI parameters but collected in both the anterior-to-posterior and posterior-to-anterior directions. These scans acquired in order to estimate and correct for distortion (Andersson et al., 2003). The 6 runs of functional data were collected while individuals were performing the PRO paradigm. As mentioned above, participants also completed 2 other tasks in the scanner, and the order of the tasks was counterbalanced.

MRI Data Pre-Processing and Analysis

medRxiv preprint doi: https://doi.org/10.1101/2020.01.20.20018069; this version posted January 27, 2020. The copyright holder has placed this preprint (which was not certified by peer review) in the Public Domain. It is no longer restricted by copyright. Anyone can legally share, reuse, remix, or adapt this material for any purpose without crediting the original authors.

Data were converted from raw DICOM images to the BIDS specification format (Gorgolewski et al., 2016) using heudiconv (v0.5.1, https://github.com/nipy/heudiconv/releases/tag/v0.5.1). Data were first preprocessed using FMRIPREP (Esteban et al., 2019), a Nipype based tool (Gorgolewski et al., 2017, 2011). FMRIPREP performs anatomical and functional preprocessing basic steps (coregistration, normalization, unwarping, noise component extraction, segmentation, skullstripping, etc.). For each participant, the T1w (T1-weighted) volume was corrected for INU (intensity non-uniformity) using N4BiasFieldCorrection v2.1.0 (Tustison et al., 2010) and skull-stripped using antsBrainExtraction.sh v2.1.0 (using the OASIS template). Brain surfaces were reconstructed using recon-all from FreeSurfer v6.0.1 (Dale et al., 1999), and the brain mask estimated previously was refined with a custom variation of the method to reconcile ANTs-derived and FreeSurfer-derived segmentations of the cortical gray-matter of Mindboggle (Abraham et al., 2014a). Spatial normalization to the ICBM 152 Nonlinear Asymmetrical template version 2009c (Fonov et al., 2009) was performed through nonlinear registration with the antsRegistration tool of ANTs v2.1.0 (Avants et al., 2008), using brain-extracted versions of both T1w volume and template. Brain tissue segmentation of cerebrospinal fluid (CSF), white-matter (WM) and gray-matter (GM) was performed on the brain-extracted T1w using fast (Zhang et al., 2001), a part of FSL (FSL v5.0.9).

Functional data were motion corrected using mcflirt (FSL v5.0.9, Jenkinson et al., 2002). Distortion correction was performed using an implementation of the TOPUP technique (Andersson et al., 2003) using 3dQwarp (AFNI v16.2.07, Cox, 1996). This was followed by co-registration to the corresponding T1w using boundary-based registration (Greve and Fischl, 2009) with 9 degrees of freedom, using bbregister (FreeSurfer v6.0.1). Motion correcting transformations, field distortion

medRxiv preprint doi: https://doi.org/10.1101/2020.01.20.20018069; this version posted January 27, 2020. The copyright holder has placed this preprint (which was not certified by peer review) in the Public Domain. It is no longer restricted by copyright. Anyone can legally share, reuse, remix, or adapt this material for any purpose without crediting the original authors.

correcting warp, BOLD-to-T1w transformation and T1w-to-template (MNI) warp were concatenated and applied in a single step using antsApplyTransforms (ANTs v2.1.0) using Lanczos interpolation. ICA-based Automatic Removal Of Motion Artifacts (AROMA) was used to create a variant of the data that is non-aggressively denoised (Pruim et al., 2015). Many internal operations of FMRIPREP use Nilearn (Abraham et al., 2014b), principally within the BOLD-processing workflow. For more details of the pipeline see https://fmriprep.readthedocs.io/en/latest/workflows.html.

Volume-based preprocessed data from FMRIPREP were then processed using CIFTIFY (v2.0.9, Dickie et al., 2019), a tool based on the Human Connectome Project (HCP) minimal preprocessing pipeline (Glasser et al., 2013). CIFTIFY allows for the processing of non-HCP datasets (i.e., data without T2w structural scans) using the Connectome Workbench (v1.3.2, https://github.com/Washington-University/workbench/releases/tag/v1.3.2). CIFTIFY used the MSMSulc method to align participants' freesurfer-derived cortical surfaces (Robinson et al., 2018, 2014). Data was minimally smoothed with a 2mm FWHM Gaussian kernel, in line with the HCP minimally preprocessing pipeline. Subsequent data analysis was conducted with the HCP Pipelines (https://github.com/Washington-University/HCPpipelines/releases/tag/v4.0.0) using FSL (v6.0.1, Smith et al., 2004), FreeSurfer (v6.0.0, Dale et al., 1999), and the Connectome Workbench (v1.3.2, https://github.com/Washington-University/workbench/releases/tag/v1.3.2).

For the analysis of the preprocessed fMRI data, we modeled rule encoding and task performance (i.e., stimuli presentation and response). To gain insight into which brain areas were most involved in rule learning and retrieval, we converted whole-brain volumes to cortical surfaces and parcellated the group-level surfaces using the Multimodal Parcellation of Glasser and colleagues

medRxiv preprint doi: https://doi.org/10.1101/2020.01.20.20018069; this version posted January 27, 2020. The copyright holder has placed this preprint (which was not certified by peer review) in the Public Domain. It is no longer restricted by copyright. Anyone can legally share, reuse, remix, or adapt this material for any purpose without crediting the original authors.

(2016) which consists of 180 regions in each hemisphere. This method has the added power of a region-of-interest analysis with high spatial sensitivity and whole-brain coverage. Specifically, first-level and second-level analyses were carried out with the TaskfMRIAnalysisBatch pipeline. All analyses were carried out on data in the CIFTI format which stores data from surfaces (vertices) and volumes (voxels) concurrently in a single file comprising a listed set of grayordinates. We conducted our analyses by parcellating each cortical surface into 180 regions using parcellation published by Glasser and colleagues (2016)MMP v1.0 cortical parcellation(2016). This parcellation approach has several advantages: instead of correcting over ~32k vertices, only 360 univariate analyses are performed, thus increasing sensitivity and statistical power; furthermore, because only minimal smoothing is applied (2 mm) there is limited blurring across regions from activated regions to adjacent, non-activated regions. Rather than restricting our analyses to *a priori* prefrontal cortical regions, we analyzed the whole MMP parcellation in order to have a hybrid region-of-interest/ whole-cortex analysis. A dense timeseries analysis was conducted using the full CIFTI grayordinate data as a confirmatory analysis, and to investigate the contributions from subcortical regions, as the MMP v1.0 parcellation does not contain subcortical regions. These results are available on BALSA and in the Supplemental Results.

In all analyses, two sets of first-level regressors were defined, one time-locked to the task instruction cue stimulus (hereafter referred to as Task Cue) and another locked to the presentation of the first of three task trials following Cole and colleagues (2010) (hereafter referred to as Trial 1 or Trial 1 Performance). The event duration for the Task Cue regressor was set to 2.76 s (i.e., the duration of cue presentation) and the event duration for the Trial 1 regressor was set to 1.84 s (i.e., the duration of stimulus presentation). Separate event files were created for novel, practiced, and

medRxiv preprint doi: https://doi.org/10.1101/2020.01.20.20018069; this version posted January 27, 2020. The copyright holder has placed this preprint (which was not certified by peer review) in the Public Domain. It is no longer restricted by copyright. Anyone can legally share, reuse, remix, or adapt this material for any purpose without crediting the original authors.

error trials; for the Task Cue regressors, errors were classified as a block where 2 or more trials were incorrect. Regressors were convolved with the double-gamma HRF, and a temporal derivative was included as an additional regressor. Prior to modeling, the timeseries was high-pass filtered to 100s. The first-level analysis was carried out using FSL v.6.0.1 FILM General Linear Model with pre-whitening turned on (Woolrich et al., 2001). Four contrasts were defined: Novel > Practiced, Practiced > Novel, Novel Only, Practiced Only. First-level modeling was carried out separately for each of the 6 runs, which were combined in a second-level fixed effects analysis. A run was only included in the second-level if it contained 3 or more correct novel or practiced blocks.

Group-level statistics were performed using Permutation Analysis of Linear Models (PALM) (PALM v115a, Winkler et al., 2014), which is capable of computing univariate and multivariate non-parametric statistics using permutations and/or sign-flipping. Four group-level contrasts were defined: HC > CHR, CHR > HC, HC Mean, CHR Mean. In addition, a separate model was set-up to calculate the mean of all subjects. To prepare the data for PALM, we concatenated the second-level participant outputs of each of the four lower-level contrasts (Novel > Practiced, Practiced > Novel, Novel Only, Practiced Only). Each of the four concatenated files was entered into a single PALM analysis as a separate input and the results were corrected across the 4 within-subject map inputs and the 4 group-level contrasts to a Family-Wise Error Rate of .05. Results were saved as $-\log_{10}(p)$, such that the minimum value considered was 1.3 (i.e., -log(.05)). For the group comparison model, a mixture of 1000 permutations and sign-flips were performed with tail approximation. To further examine within and between group effects, we examined Cohen's d maps saved by PALM (-saveglm option).

Results

medRxiv preprint doi: https://doi.org/10.1101/2020.01.20.20018069; this version posted January 27, 2020. The copyright holder has placed this preprint (which was not certified by peer review) in the Public Domain. It is no longer restricted by copyright. Anyone can legally share, reuse, remix, or adapt this material for any purpose without crediting the original authors.

Behavioral Results

We were interested in whether the HC and CHR participants learned at different rates during the practice session, as a group difference during training might account for how well the brain represented the practiced tasks. For the practice session, there was a large effect of block, with accuracy increasing over the course of training ($F(4.59,201.98)=28.0$, $p<.001$, $\eta^2_p=0.39$) and reaction time decreasing ($F(3.16,138.94)=14.2$, $p<.001$, $\eta^2_p=0.24$). While there was no interaction of block and group for accuracy ($F(4.59,201.98)=0.42$, $p=.82$, $\eta^2_p=0.01$), the HC group showed a larger increase in reaction time compared to the CHR group ($F(3.16,138.94)=3.03$, $p=.029$, $\eta^2_p=0.065$).

During the scanning session, participants responded to novel tasks more slowly and less accurately compared to practiced tasks (Reaction time: $F(45)=5.62$, $p<.001$, Cohen's d=0.83; Accuracy: Wilcoxon $W=245$, $p<.004$, Cohen's d=-0.48). However, there was no interaction of task type and group (Reaction time: $F(1,44)=0.04$, $p=.84$, $\eta^2_p=0.001$; Accuracy: $F(1,44)=0.65$, $p=.42$, $\eta^2_p=0.02$). To examine whether there was further learning during the scanning session, we analyzed behavior over the course of the six scanner blocks. While participants became faster over the course of the scanning session ($F(4.05, 174.36)=8.6$, $p<.001$, $\eta^2_p=0.167$), there was no block by task type interaction ($F(4.01, 172.56)=0.81$ $p=.52$, $\eta^2_p=0.018$). Accuracy did not differ by block ($F(4.01, 176.44)=1.47$ $p=.21$, $\eta^2_p=0.03$). There were no effects with group for reaction time (all F's < 0.81) or accuracy (all F's < 0.48). Descriptive statistics are reported in Table 2 (reaction times) and Table 3 (accuracy).

Imaging Results

medRxiv preprint doi: https://doi.org/10.1101/2020.01.20.20018069; this version posted January 27, 2020. The copyright holder has placed this preprint (which was not certified by peer review) in the Public Domain. It is no longer restricted by copyright. Anyone can legally share, reuse, remix, or adapt this material for any purpose without crediting the original authors.

Group-level Permutation Statistics

We first examined brain activation during task cue encoding and task performance with parcel-wise permutation statistical testing. As no parcels showed any significant differences in the contrast between novel and practiced tasks, we examined which parcels were significantly active in each condition alone (see Figure 2). While Cole and colleagues (2010) found that novel task encoding activated the DLPFC and practiced task encoding activated the RLPFC, here we found overlapping activation across the brain, including regions of anterior (9/46d), middle (46, 9/46v), and posterior prefrontal cortex (IFSp, IFJa, 8C). Novel and practiced task cues also yielded overlapping activation in the striatum and cerebellum. During task performance, the healthy controls again did not show the differential activation observed by Cole and colleagues, with overlapping activation of middle and posterior lateral PFC for both novel and practiced tasks. See Supplemental Figure 1 for lateral and medial surface results from both hemispheres and Supplemental Figure 2 for the subcortical results from the dense timeseries analysis.

While the CHR group also did not demonstrate any significant differences between novel and practiced task during encoding and task performance, there were qualitative differences in the patterns of activation, as shown in Figure 2. The CHR group showed the opposite pattern as Cole and colleagues (2010), with RLPFC (9-46d) activation by novel, but not practiced task cue encoding; for practiced task cue encoding, CHR showed activation of posterior ventrolateral PFC (VLPFC). Moreover, during task performance the CHR group showed activation of anterior VLPFC regions that were not active in the HC group; specifically, CHR participants showed activation of area 47r and area 45. See Supplemental Figure 1 for lateral and medial surface results from both hemispheres and Supplemental Figure 2 for subcortical results from the dense timeseries analysis.

medRxiv preprint doi: https://doi.org/10.1101/2020.01.20.20018069; this version posted January 27, 2020. The copyright holder has placed this preprint (which was not certified by peer review) in the Public Domain. It is no longer restricted by copyright. Anyone can legally share, reuse, remix, or adapt this material for any purpose without crediting the original authors.

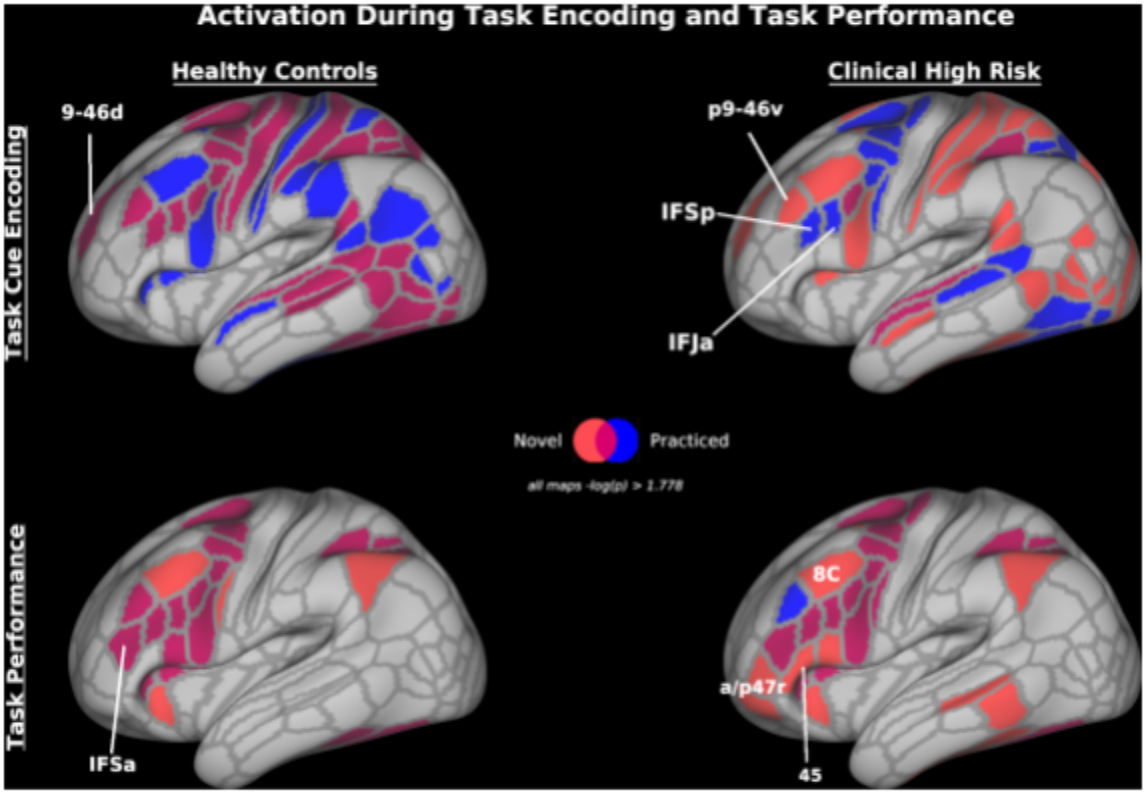

Figure 2. Activation during novel and practiced tasks at task cue encoding and task performance. Results are corrected at the parcel level with permutation testing to a threshold of -log(p) > 1.778 (equivalent to p<.05 with Bonferroni correction for 3 tests: Left Cortical Surface, Right Cortical Surface, subcortical dense volume). Outlines depict the boundaries of the Glasser et al. Multi-modal Parcellation [91], and labels come from that parcellation. Novel trial activation is shown in red, practiced task activation is shown in blue, and overlapping activation is shown in purple. Lateral and medial cortical surfaces of both hemispheres are shown in Supplemental Figure 1, and subcortical volumes are shown in Supplemental Figure 2.

Group-level effect size comparison

Since there were no significant results in the contrasts of novel and practiced trials, we examined the Cohen's d effect size maps for the contrasts of novel and practiced task trials (see Figure 3). These would indicate whether or not the design simply did not have enough power to identify significant effects. Partially supporting Cole and colleagues (2013a, 2010), in the HC group, there was a small effect in the RLPFC during task encoding for the contrast of practiced > novel, and a moderate effect in the RLPFC during task performance for the contrast of novel > practiced.

medRxiv preprint doi: https://doi.org/10.1101/2020.01.20.20018069; this version posted January 27, 2020. The copyright holder has placed this preprint (which was not certified by peer review) in the Public Domain. It is no longer restricted by copyright. Anyone can legally share, reuse, remix, or adapt this material for any purpose without crediting the original authors.

However, there was a dorsal-ventral split for task cue encoding and task performance, respectively; this has not been demonstrated with this task before. Furthermore, as supported by the statistical comparison shown in Figure 2, there was no effect of the contrast of novel and practiced tasks in the DLPFC, suggesting that this area was equally involved in novel and practiced task encoding and performance. Unexpectedly, the CHR group showed a small effect in the RLPFC for novel vs. practiced task encoding. The CHR group did not show any notable effects for the comparison of practiced vs. novel trials during either encoding or task performance.

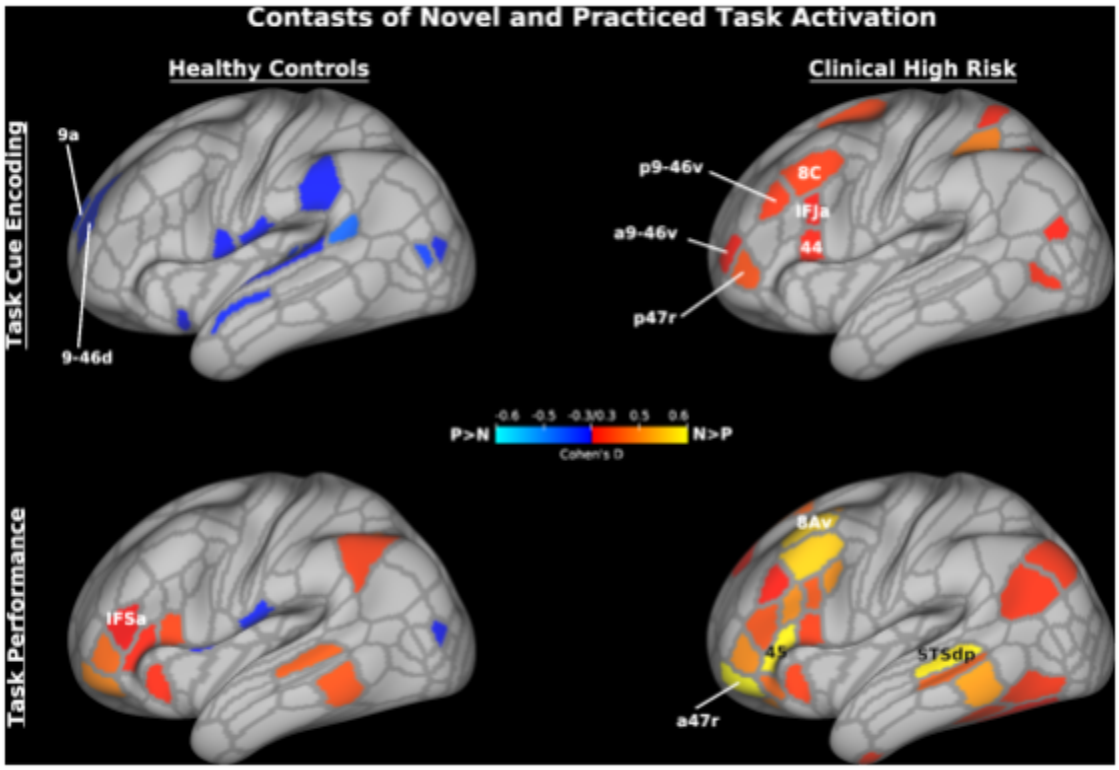

Figure 3. Effect size maps of contrasts of novel and practiced tasks at task cue encoding and task performance. The contrast of novel > practiced is shown in hot colors and the contrast of practiced > novel is shown in cold colors. Values shown are Cohen's D with a minimum threshold of 0.3. Lateral and medial cortical surfaces of both hemispheres are shown in Supplemental Figure 3 and subcortical volumes are shown in Supplemental Figure 4.

We then examined the effect size for the between group comparisons. As shown in Figure 4, during task cue encoding, the prefrontal cortex showed small to large effects for the contrast of

medRxiv preprint doi: https://doi.org/10.1101/2020.01.20.20018069; this version posted January 27, 2020. The copyright holder has placed this preprint (which was not certified by peer review) in the Public Domain. It is no longer restricted by copyright. Anyone can legally share, reuse, remix, or adapt this material for any purpose without crediting the original authors.

HC>CHR. The largest effects were observed in the DLPFC for practiced tasks. As shown in Figure 4 and Supplemental Figure 7, controls showed large effects of activation across a number of key networks, including the fronto-parietal control network, motor regions, and higher-level visual regions, suggesting that controls were better at proactive control to prepare for a practiced task. The majority of regions with effects for the contrast of CHR>HC were observed during task performance; the regions with the largest effect were 10d, 9p, a9-46v, and 8Av. Notably, these regions were absent in the HC group, as shown in Figures 2 and 3.

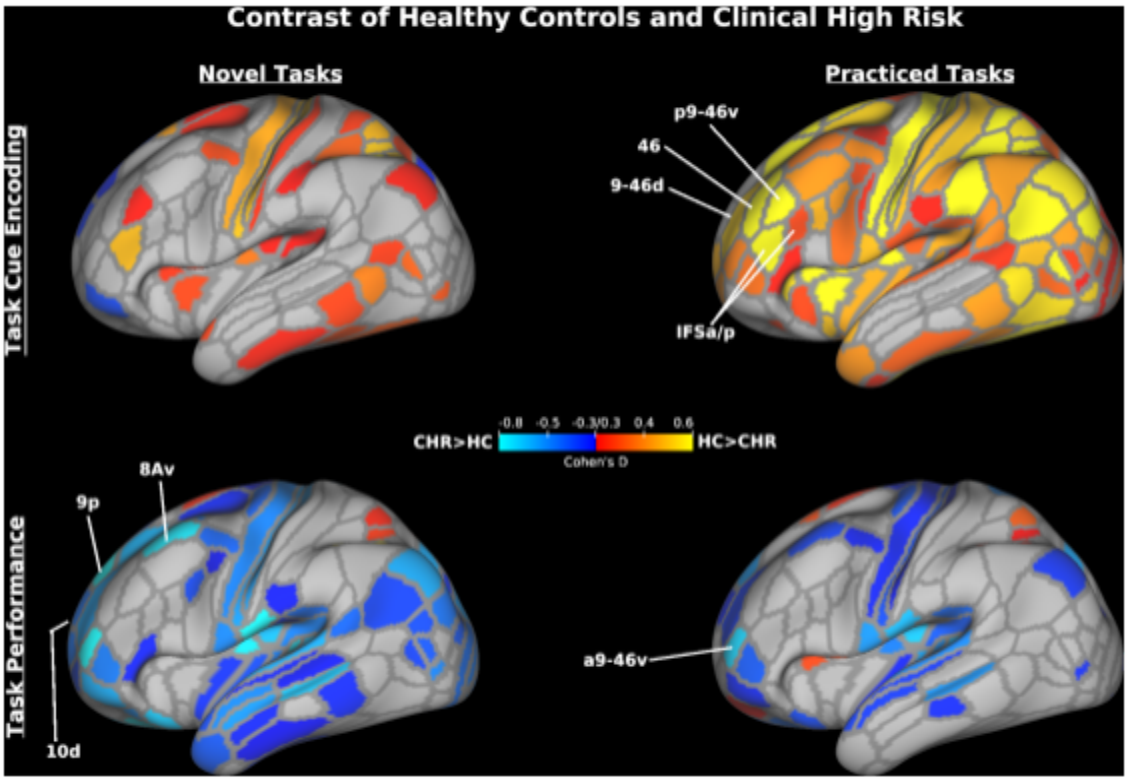

Figure 4. Effect size maps of contrasts of the Healthy Control (HC) group and the Clinical High Risk (CHR) group for novel and practiced tasks at task cue encoding and task performance. The contrast of Novel > Practiced is shown in hot colors and the contrast of Practiced > Novel is shown in cold colors. Values shown are Cohen's D with a minimum threshold of 0.3. Lateral and medial cortical surfaces of both hemispheres are shown in Supplemental Figure 5, and subcortical volumes are shown in Supplemental Figure 6.

medRxiv preprint doi: https://doi.org/10.1101/2020.01.20.20018069; this version posted January 27, 2020. The copyright holder has placed this preprint (which was not certified by peer review) in the Public Domain. It is no longer restricted by copyright. Anyone can legally share, reuse, remix, or adapt this material for any purpose without crediting the original authors.

Discussion

In the current study we investigated rapid instructed task learning (RITL) in a group of adolescents at clinical high risk (CHR) for psychosis and a group of healthy control (HC) participants. Participants were required to quickly encode a set of rules into a goal set and then maintain this goal set to perform a series of trials (Cole et al., 2010). While previous studies have demonstrated that a disability in representing goal information is central to schizophrenia (Barch and Ceaser, 2012), it has been unclear if this deficit begins before or after the onset of schizophrenia. Moreover, previous fMRI studies of goal maintenance is psychosis have focused on well learned tasks while in our day to day lives we may have to adapt previously acquired rules to new tasks and contexts. While no statistically significant group differences were identified, we identified moderate-to-large sized effects suggesting that CHR participants show poor task rule encoding, and rely on less effective reactive control mechanisms to apply task rules during task performance. Overall, this is a novel investigation of the course of goal maintenance deficits in psychosis and the first study of rapid task learning in psychosis.

Rapid Instructed Task Learning in Controls

In healthy controls, we aimed to replicate previous findings by Cole and colleagues (2016, 2010) demonstrating a reversal of prefrontal brain dynamics for practiced and novel task encoding and performance. Cole and colleagues found that novel task rules are first encoded by the DLPFC and then integrated into working memory by the RLPFC; these dynamics are reversed for practiced tasks, with rules being retrieved from long-term memory by the RLPFC and then activated by DLPFC working memory mechanisms for task performance. Using high-resolution, ultra-fast

medRxiv preprint doi: https://doi.org/10.1101/2020.01.20.20018069; this version posted January 27, 2020. The copyright holder has placed this preprint (which was not certified by peer review) in the Public Domain. It is no longer restricted by copyright. Anyone can legally share, reuse, remix, or adapt this material for any purpose without crediting the original authors.

multiband fMRI sequences and cutting-edge analysis techniques developed by the Human Connectome Project, we partially replicated this pattern in healthy controls, and identified some critical deviations.

When we examined the thresholded statistical maps in the current study, we found no statistically significant differences in activation for the contrast of novel vs. practiced tasks. Compared to baseline, novel and practiced tasks both showed significant activation of the RLPFC and DLPFC during task cue encoding and DLPFC and VLPFC activation during task performance. However, when we looked at the effect size maps (Cohen's D), the controls showed a small effect of greater RLPFC activation for practiced vs. novel task cue encoding. If the novel rules were truly represented as distinct from practiced rules, we would expect to see greater activation of brain areas involved in switching rules or switching tasks (Cole et al., 2010). Switching of tasks or task sets has been suggested to rely on regions of the lateral prefrontal cortex (primarily DLPFC and IFJ) as well as the intraparietal sulcus (IPS) (Kim et al., 2012). Rule switching, however, has been suggested to rely on medial rather than lateral prefrontal cortex (Crone et al., 2005). MVPA decoding work has shown that specific task rules are first encoded in the IPS, though this is likely to be true primarily for practice rules (Bode and Haynes, 2009). Nevertheless, in the current study, there was little evidence to suggest a difference in how the novel and practiced rules were encoded.

The task performance data deviated further from the findings of Cole and colleagues. As with the task cue encoding results, we found no statistically significant difference between novel and practiced task performance. While the effect size maps showed small-to-medium sized effects for the contrast of Novel>Practiced, the effect was found in the anterior VLPFC. This region has been associated with general retrieval of rules from long-term memory (Cole et al., 2010; Donohue et al.,

medRxiv preprint doi: https://doi.org/10.1101/2020.01.20.20018069; this version posted January 27, 2020. The copyright holder has placed this preprint (which was not certified by peer review) in the Public Domain. It is no longer restricted by copyright. Anyone can legally share, reuse, remix, or adapt this material for any purpose without crediting the original authors.

2005) as well as the need to control such retrieval mechanisms (Badre and Wagner, 2004). Supporting this role for the anterior VLPFC, we found the same effect in the middle temporal cortex. While we predicted that such retrieval mechanisms would be involved during task cue encoding, particularly for practiced tasks, it was surprising to see possible retrieval during task performance. One possibility is that participants retrieved instances from practiced task trials in order to determine how to apply the novel rule. For instance, participants may have practiced judging the sweetness of the stimuli or applying the logic rule of both stimuli requiring the same semantic label, and drew upon those instances to apply a novel task set. In support of this possibility, behavioral responses to novel tasks were slower and less accurate compared to practiced tasks, allowing for such a late, reactive control process to occur. As noted elsewhere, the psychological need for short cue-to-target intervals in typical task switching designs has made it difficult to separate preparatory activity locked to the cue and reactive activity locked to the target presentation (Ruge et al., 2013).

These functional dynamics in the lateral prefrontal cortex observed during RITL are demonstrative of theories of functional brain organization. The lateral prefrontal cortex is thought to be organized along a rostral-to-caudal abstraction gradient; rostral regions control more abstract, domain general processing, while caudal regions control for more concrete, domain specific processing (Badre, 2008; Nee and D'Esposito, 2016). While earlier work suggested that this gradient was hierarchical, with the RLPFC lying at the apex (Christoff and Gabrieli, 2000; Koechlin et al., 2003; Koechlin and Summerfield, 2007), other work has demonstrated that the subregions of the lateral prefrontal cortex can act relatively independently (Crittenden and Duncan, 2012; Kim et al.,

medRxiv preprint doi: https://doi.org/10.1101/2020.01.20.20018069; this version posted January 27, 2020. The copyright holder has placed this preprint (which was not certified by peer review) in the Public Domain. It is no longer restricted by copyright. Anyone can legally share, reuse, remix, or adapt this material for any purpose without crediting the original authors.

2012). An alternative view suggests that the DLPFC, rather that the RLPFC, is the apex of a prefrontal hierarchy (Badre and Nee, 2017). Similarly, work by Cole and colleagues (2017, 2013b) has demonstrated that flexibility in task performance relies on the ability of the DLPFC to flexibly change its connectivity depending on task parameters. Thus, the DLPFC appears to play a critical role in flexible task performance (like in the RITL), supported by other regions like the RLPFC.

Task Learning Deficits in Psychosis Risk

Despite the lack of a statistical group effect, there were medium-to-large effects for the comparison of the HC and CHR groups during both task cue encoding and task performance. The difference was most apparent for practiced task encoding. The large effect size of the group difference across the DLPFC, middle VLPFC, and IPS suggests that CHR participants showed deficient retrieval and maintenance of learned task rules. This is despite the lack of a difference in performance during the practice session. These findings are in line with previous studies showing poor proactive control and goal maintenance in schizophrenia in conjunction with deficits in prefrontal functioning (Barch and Ceaser, 2012; Poppe et al., 2016; Sheffield et al., 2014). Although less prevalent in the group comparison, the CHR group appeared to rely on reactive control mechanisms, in particular for novel task performance. Lesh and colleagues (2013) found that first-episode schizophrenia was associated with hypoactivation of the DLPFC during proactive control, but normal activation during reactive control. Reactive control has also been shown to be intact in schizophrenia in instances of motivated control in response to reward (Mann et al., 2013). Nevertheless, patients with schizophrenia show diminished activation of control regions at longer RTs, which has been suggested to reflect deficits of reactive control mechanisms needed to overcome lapses of proactive control (Fassbender et al., 2014). However, further research is needed

medRxiv preprint doi: https://doi.org/10.1101/2020.01.20.20018069; this version posted January 27, 2020. The copyright holder has placed this preprint (which was not certified by peer review) in the Public Domain. It is no longer restricted by copyright. Anyone can legally share, reuse, remix, or adapt this material for any purpose without crediting the original authors.

to elucidate whether the activation of frontal and parietal control regions during task performance, as opposed to during cue encoding actually reflects reactive control.

Overall, the results suggest that the Clinical High Risk stage of psychosis is associated with similar, albeit less pronounced, deficits in goal maintenance and task set learning that are observed in schizophrenia. It has been suggested that schizophrenia patients may use inefficient encoding and retrieval strategies compared to healthy controls (MacDonald et al., 2005). This may be due to a breakdown in networks that support the integration of long-term memory and working memory (Ragland et al., 2012). Although the CHR group may not have shown any reductions in activity during novel task encoding, the results suggest that the instructions were not encoding correctly, forcing them to rely on retrieval mechanisms during task performance, rather than more efficient preparatory control.

Limitations and Future Directions

Although our sample size was in line with recent studies of executive function in psychosis, the disparity between the effect size and the lack of significant group-level effects suggests that additional participants are needed. We used a recently developed parcellation approach which added power without losing spatial coverage. To this end, we were able to investigate the contributions of prefrontal subregions to executive functions. Although we adapted the task previously used by Cole and colleagues (2013a, 2010), we used a different analysis approach. Cole and colleagues first identified regions within the prefrontal cortex that showed a condition (practiced vs. novel) X time interaction with a liberal cluster formation threshold and then performed ANOVAs on regions of interest to identify region X condition interactions during the encoding and task performance periods. We performed a single parcellated analysis to avoid any biases in ROI selection and did not

medRxiv preprint doi: https://doi.org/10.1101/2020.01.20.20018069; this version posted January 27, 2020. The copyright holder has placed this preprint (which was not certified by peer review) in the Public Domain. It is no longer restricted by copyright. Anyone can legally share, reuse, remix, or adapt this material for any purpose without crediting the original authors.

employ a Finite Impulse Response model as used by Cole and colleagues. Nevertheless, our effect size maps suggest that even with a different analysis strategy, neither the HC or CHR participants would show the pattern of results demonstrated by Cole and colleagues. Future studies should investigate whether psychosis risk participants show deficits in rule learning using different paradigms such as those developed by Dumontheil and colleagues (2011).

medRxiv preprint doi: https://doi.org/10.1101/2020.01.20.20018069; this version posted January 27, 2020. The copyright holder has placed this preprint (which was not certified by peer review) in the Public Domain. It is no longer restricted by copyright. Anyone can legally share, reuse, remix, or adapt this material for any purpose without crediting the original authors.

Acknowledgements

We are grateful to Tina Gupta for assistance with participant recruitment and to Derek Dean and all of the research assistants at the CU ADAPT Program for their help with running participants. E-Prime file for the paradigm were graciously provided by Michael W. Cole. This work was funded by the National Institute of Mental Health R01MH094650 to V.A.M.. J.M.O. was supported by F32DA034412 and by start-up funds from Texas A&M University. J.A.B. was supported by NIH F32MH102898, a Brain & Behavior Research Foundation NARSAD Young Investigator Award as the Donald & Janet Boardman Family Investigator, and by start-up funds from Texas A&M University.

medRxiv preprint doi: https://doi.org/10.1101/2020.01.20.20018069; this version posted January 27, 2020. The copyright holder has placed this preprint (which was not certified by peer review) in the Public Domain. It is no longer restricted by copyright. Anyone can legally share, reuse, remix, or adapt this material for any purpose without crediting the original authors.

Disclosures

VAM is a consultant to Takeda Pharmaceuticals. The other authors report no biomedical financial interests or potential conflicts of interest.

medRxiv preprint doi: https://doi.org/10.1101/2020.01.20.20018069; this version posted January 27, 2020. The copyright holder has placed this preprint (which was not certified by peer review) in the Public Domain. It is no longer restricted by copyright. Anyone can legally share, reuse, remix, or adapt this material for any purpose without crediting the original authors.

References

Abraham, A., Dohmatob, E., Thirion, B., Samaras, D., Varoquaux, G., 2014a. Region segmentation for sparse decompositions: better brain parcellations from rest fMRI. arXiv [q-bio.NC].

Abraham, A., Pedregosa, F., Eickenberg, M., Gervais, P., Mueller, A., Kossaifi, J., Gramfort, A., Thirion, B., Varoquaux, G., 2014b. Machine learning for neuroimaging with scikit-learn. Front. Neuroinform. 8, 14. https://doi.org/10.3389/fninf.2014.00014

Allen, P., Luigjes, J., Howes, O.D., Egerton, A., Hirao, K., Valli, I., Kambeitz, J., Fusar-Poli, P., Broome, M., McGuire, P., 2012. Transition to psychosis associated with prefrontal and subcortical dysfunction in ultra high-risk individuals. Schizophr. Bull. 38, 1268–1276. https://doi.org/10.1093/schbul/sbr194

Amminger, G.P., Paul Amminger, G., Schäfer, M.R., McGorry, P.D., 2010. WHO RESPONDS TO TREATMENT WITH OMEGA-3 FATTY ACID? FINDINGS FROM AN INDICATED PREVENTION TRIAL IN YOUNG PEOPLE AT ULTRA-HIGH RISK OF PSYCHOSIS. Schizophrenia Research. https://doi.org/10.1016/j.schres.2010.02.453

Andersson, J.L.R., Skare, S., Ashburner, J., 2003. How to correct susceptibility distortions in spin-echo echo-planar images: Application to diffusion tensor imaging. Neuroimage 20, 870–888. https://doi.org/10.1016/S1053-8119(03)00336-7

Avants, B.B., Epstein, C.L., Grossman, M., Gee, J.C., 2008. Symmetric diffeomorphic image registration with cross-correlation: evaluating automated labeling of elderly and neurodegenerative brain. Med. Image Anal. 12, 26–41. https://doi.org/10.1016/j.media.2007.06.004

Badre, D., 2008. Cognitive control, hierarchy, and the rostro–caudal organization of the frontal lobes. Trends Cogn. Sci. 12, 193–200. https://doi.org/10.1016/j.tics.2008.02.004

Badre, D., Nee, D.E., 2017. Frontal Cortex and the Hierarchical Control of Behavior. Trends Cogn. Sci. 22, 170–188. https://doi.org/10.1016/j.tics.2017.11.005

Badre, D., Wagner, A.D., 2004. Selection, integration, and conflict monitoring; assessing the nature and generality of prefrontal cognitive control mechanisms. Neuron 41, 473–487.

Barch, D.M., Ceaser, A., 2012. Cognition in schizophrenia: core psychological and neural mechanisms. Trends Cogn. Sci. 16, 27–34. https://doi.org/10.1016/j.tics.2011.11.015

Bode, S., Haynes, J.-D., 2009. Decoding sequential stages of task preparation in the human brain. Neuroimage 45, 606–613. https://doi.org/10.1016/j.neuroimage.2008.11.031

Bora, E., Murray, R.M., 2014. Meta-analysis of Cognitive Deficits in Ultra-high Risk to Psychosis and First-Episode Psychosis: Do the Cognitive Deficits Progress Over, or After, the Onset of Psychosis? Schizophrenia Bulletin. https://doi.org/10.1093/schbul/sbt085

Braver, T.S., Barch, D.M., 2006. Extracting core components of cognitive control. Trends Cogn. Sci. 10, 529–532. https://doi.org/10.1016/j.tics.2006.10.006

Camchong, J., Lim, K.O., Sponheim, S.R., Macdonald, A.W., 2009. Frontal white matter integrity as an endophenotype for schizophrenia: diffusion tensor imaging in monozygotic twins and patients' nonpsychotic relatives. Front. Hum. Neurosci. 3, 35. https://doi.org/10.3389/neuro.09.035.2009

Cannon, T.D., Cadenhead, K., Cornblatt, B., Woods, S.W., Addington, J., Walker, E., Seidman, L.J., Perkins, D., Tsuang, M., McGlashan, T., Heinnsen, R., 2008. Prediction of Psychosis in youth at High Clinical Risk. Arch. Gen. Psychiatry 65, 28–37.

Cannon, T.D., Yu, C., Addington, J., Bearden, C.E., Cadenhead, K.S., Cornblatt, B.A., Heinssen, R., Jeffries, C.D., Mathalon, D.H., McGlashan, T.H., Perkins, D.O., Seidman, L.J., Tsuang, M.T., Walker, E.F., Woods, S.W., Kattan, M.W., 2016. An individualized risk calculator for research in prodromal psychosis. Am. J. Psychiatry 173, 980–988. https://doi.org/10.1176/appi.ajp.2016.15070890

Carrión, R.E., Walder, D.J., Auther, A.M., McLaughlin, D., Zyla, H.O., Adelsheim, S., Calkins, R., Carter, C.S., McFarland, B., Melton, R., Niendam, T., Ragland, J.D., Sale, T.G., Taylor, S.F., McFarlane, W.R.,

medRxiv preprint doi: https://doi.org/10.1101/2020.01.20.20018069; this version posted January 27, 2020. The copyright holder has placed this preprint (which was not certified by peer review) in the Public Domain. It is no longer restricted by copyright. Anyone can legally share, reuse, remix, or adapt this material for any purpose without crediting the original authors.

Cornblatt, B.A., 2018. From the psychosis prodrome to the first-episode of psychosis: No evidence of a cognitive decline. J. Psychiatr. Res. 96, 231–238. https://doi.org/10.1016/j.jpsychires.2017.10.014

Christoff, K., Gabrieli, J.D.E., 2000. The frontopolar cortex and human cognition: Evidence for a rostrocaudal hierarchical organization within the human prefrontal cortex. Psychobiology 28, 168–186. https://doi.org/10.3758/BF03331976

Cloutier, M., Aigbogun, M.S., Guerin, A., Nitulescu, R., Ramanakumar, A.V., Kamat, S.A., DeLucia, M., Duffy, R., Legacy, S.N., Henderson, C., Francois, C., Wu, E., 2016. The Economic Burden of Schizophrenia in the United States in 2013. J. Clin. Psychiatry 77, 764–771. https://doi.org/10.4088/JCP.15m10278

Cole, M.W., Bagic, A., Kass, R., Schneider, W., 2010. Prefrontal dynamics underlying rapid instructed task learning reverse with practice. Journal of Neuroscience 30, 14245–14254. https://doi.org/10.1523/JNEUROSCI.1662-10.2010

Cole, M.W., Braver, T.S., Meiran, N., 2017. The task novelty paradox: Flexible control of inflexible neural pathways during rapid instructed task learning. Neurosci. Biobehav. Rev. 81, 4–15. https://doi.org/10.1016/j.neubiorev.2017.02.009

Cole, M.W., Ito, T., Braver, T.S., 2016. The Behavioral Relevance of Task Information in Human Prefrontal Cortex. Cereb. Cortex 1–9. https://doi.org/10.1093/cercor/bhv072

Cole, M.W., Laurent, P., Stocco, A., 2013a. Rapid instructed task learning: a new window into the human brain's unique capacity for flexible cognitive control. Cogn. Affect. Behav. Neurosci. 13, 1–22. https://doi.org/10.3758/s13415-012-0125-7

Cole, M.W., Reynolds, J.R., Power, J.D., Repovs, G., Anticevic, A., Braver, T.S., 2013b. Multi-task connectivity reveals flexible hubs for adaptive task control. Nat. Neurosci. 16. https://doi.org/10.1038/nn.3470

Corcoran, C.M., First, M.B., Cornblatt, B., 2010. The psychosis risk syndrome and its proposed inclusion in the DSM-V: A risk–benefit analysis. Schizophr. Res. 120, 16–22. https://doi.org/10.1016/j.schres.2010.03.018

Cox, R.W., 1996. AFNI: Software for analysis and visualization of functional magnetic resonance neuroimages. Comput. Biomed. Res. 29, 162–173.

Crittenden, B.M., Duncan, J., 2012. Task difficulty manipulation reveals multiple demand activity but no frontal lobe hierarchy. Cereb. Cortex 24, 532–540.

Crone, E.A., Wendelken, C., Donohue, S.E., Bunge, S.A., 2005. Neural evidence for dissociable components of task-switching. Cereb. Cortex 16, 475–486.

Dale, A.M., Fischl, B., Sereno, M.I., 1999. Cortical surface-based analysis. I. Segmentation and surface reconstruction. Neuroimage 9, 179–194. https://doi.org/10.1006/nimg.1998.0395

Damme, K.S.F., Gupta, T., Nusslock, R., Bernard, J.A., Orr, J.M., Mittal, V.A., 2019a. Cortical Morphometry in the Psychosis Risk Period: A Comprehensive Perspective of Surface Features. Biol Psychiatry Cogn Neurosci Neuroimaging 4, 434–443. https://doi.org/10.1016/j.bpsc.2018.01.003

Damme, K.S.F., Pelletier-Baldelli, A., Cowan, H.R., Orr, J.M., Mittal, V.A., 2019b. Distinct and opposite profiles of connectivity during self-reference task and rest in youth at clinical high risk for psychosis. Hum. Brain Mapp. hbm.24595. https://doi.org/10.1002/hbm.24595

Dickie, E.W., Anticevic, A., Smith, D.E., Coalson, T.S., Manogaran, M., Calarco, N., Viviano, J.D., Glasser, M.F., Van Essen, D.C., Voineskos, A.N., 2019. Ciftify: A framework for surface-based analysis of legacy MR acquisitions. Neuroimage 197, 818–826. https://doi.org/10.1016/j.neuroimage.2019.04.078

Donohue, S.E., Wendelken, C., Crone, E.A., Bunge, S.A., 2005. Retrieving rules for behavior from long-term memory. NeuroImage. https://doi.org/10.1016/j.neuroimage.2005.03.019

Dumontheil, I., Thompson, R., Duncan, J., 2011. Assembly and use of new task rules in fronto-parietal cortex. J. Cogn. Neurosci. 23, 168–182. https://doi.org/10.1162/jocn.2010.21439

Duncan, J., 2010. The multiple-demand (MD) system of the primate brain: mental programs for intelligent

medRxiv preprint doi: https://doi.org/10.1101/2020.01.20.20018069; this version posted January 27, 2020. The copyright holder has placed this preprint (which was not certified by peer review) in the Public Domain. It is no longer restricted by copyright. Anyone can legally share, reuse, remix, or adapt this material for any purpose without crediting the original authors.

behaviour. Trends Cogn. Sci. 14, 172–179. https://doi.org/10.1016/j.tics.2010.01.004

Duncan, J., 1986. Disorganisation of behavior after frontal lobe damage. Cogn. Neuropsychol. 3, 271–290.

Esteban, O., Markiewicz, C.J., Blair, R.W., Moodie, C.A., Isik, A.I., Erramuzpe, A., Kent, J.D., Goncalves, M., DuPre, E., Snyder, M., Oya, H., Ghosh, S.S., Wright, J., Durnez, J., Poldrack, R.A., Gorgolewski, K.J., 2019. fMRIPrep: a robust preprocessing pipeline for functional MRI. Nat. Methods 16, 111–116. https://doi.org/10.1038/s41592-018-0235-4

Fassbender, C., Scangos, K., Lesh, T.A., Carter, C.S., 2014. RT distributional analysis of cognitive-control-related brain activity in first-episode schizophrenia. Cogn. Affect. Behav. Neurosci. 14, 175–188. https://doi.org/10.3758/s13415-014-0252-4

First, M., Spitzer, R., Gibbon, M., Williams, J., 1995. Structured Clinical Interview for the DSM-IV Axis I Disorders (SCID-I), Patient Edition. American Psychiatric Press, Washington DC.

Fisher, M., Loewy, R., Hardy, K., Schlosser, D., Vinogradov, S., 2013. Cognitive interventions targeting brain plasticity in the prodromal and early phases of schizophrenia. Annu. Rev. Clin. Psychol. 9, 435–463. https://doi.org/10.1146/annurev-clinpsy-032511-143134

Fonov, V.S., Evans, A.C., McKinstry, R.C., Almli, C.R., Collins, D.L., 2009. Unbiased nonlinear average age-appropriate brain templates from birth to adulthood. Neuroimage 47, S102. https://doi.org/10.1016/S1053-8119(09)70884-5

Fornito, A., Harrison, B.J., Goodby, E., Dean, A., Ooi, C., Nathan, P.J., Lennox, B.R., Jones, P.B., Suckling, J., Bullmore, E.T., 2013. Functional dysconnectivity of corticostriatal circuitry as a risk phenotype for psychosis. JAMA Psychiatry 70, 1143–1151. https://doi.org/10.1001/jamapsychiatry.2013.1976

Fusar-Poli, P., Cappucciati, M., Borgwardt, S., Woods, S.W., Addington, J., Nelson, B., Nieman, D.H., Stahl, D.R., Rutigliano, G., Riecher-Rössler, A., Simon, A.E., Mizuno, M., Lee, T.Y., Kwon, J.S., Lam, M.M.L., Perez, J., Keri, S., Amminger, P., Metzler, S., Kawohl, W., Rössler, W., Lee, J., Labad, J., Ziermans, T., An, S.K., Liu, C.-C., Woodberry, K.A., Braham, A., Corcoran, C., McGorry, P., Yung, A.R., McGuire, P.K., 2016. Heterogeneity of Psychosis Risk Within Individuals at Clinical High Risk: A Meta-analytical Stratification. JAMA Psychiatry 73, 113–120. https://doi.org/10.1001/jamapsychiatry.2015.2324

Fusar-Poli, P., Deste, G., Smieskova, R., Barlati, S., Yung, A.R., Howes, O., Stieglitz, R.-D., Vita, A., McGuire, P., Borgwardt, S., 2012. Cognitive functioning in prodromal psychosis: a meta-analysis. Arch. Gen. Psychiatry 69, 562–571. https://doi.org/10.1001/archgenpsychiatry.2011.1592

Fusar-Poli, P., Howes, O.D., Allen, P., Broome, M., Valli, I., Asselin, M.-C., Montgomery, A.J., Grasby, P.M., McGuire, P., 2011. Abnormal prefrontal activation directly related to pre-synaptic striatal dopamine dysfunction in people at clinical high risk for psychosis. Mol. Psychiatry 16, 67–75. https://doi.org/10.1038/mp.2009.108

Fusar-Poli, P., McGuire, P., Borgwardt, S., 2012. Mapping prodromal psychosis: a critical review of neuroimaging studies. Eur. Psychiatry 27, 181–191. https://doi.org/10.1016/j.eurpsy.2011.06.006

Glasser, M.F., Coalson, T.S., Robinson, E.C., Hacker, C.D., Harwell, J., Yacoub, E., Ugurbil, K., Andersson, J., Beckmann, C.F., Jenkinson, M., Smith, S.M., Van Essen, D.C., 2016. A multi-modal parcellation of human cerebral cortex. Nature 536, 171–178. https://doi.org/10.1038/nature18933

Glasser, M.F., Sotiropoulos, S.N., Wilson, J.A., Coalson, T.S., Fischl, B., Andersson, J.L.R., Xu, J., Jbabdi, S., Webster, M., Polimeni, J.R., Van Essen, D.C., Jenkinson, M., 2013. The minimal preprocessing pipelines for the human connectome project. Neuroimage 80, 105–124. https://doi.org/10.1016/j.neuroimage.2013.04.127

Gorgolewski, K.J., Auer, T., Calhoun, V.D., Craddock, R.C., Das, S., Duff, E.P., Flandin, G., Ghosh, S.S., Glatard, T., Halchenko, Y.O., Handwerker, D.A., Hanke, M., Keator, D., Li, X., Michael, Z., Maumet, C., Nichols, B.N., Nichols, T.E., Pellman, J., Poline, J.-B., Rokem, A., Schaefer, G., Sochat, V., Triplett, W., Turner, J.A., Varoquaux, G., Poldrack, R.A., 2016. The brain imaging data structure, a format for organizing and describing outputs of neuroimaging experiments. Sci Data 3, 160044. https://doi.org/10.1038/sdata.2016.44

medRxiv preprint doi: https://doi.org/10.1101/2020.01.20.20018069; this version posted January 27, 2020. The copyright holder has placed this preprint (which was not certified by peer review) in the Public Domain. It is no longer restricted by copyright. Anyone can legally share, reuse, remix, or adapt this material for any purpose without crediting the original authors.

Gorgolewski, K.J., Burns, C.D., Madison, C., Clark, D., Halchenko, Y.O., Waskom, M.L., Ghosh, S.S., 2011. Nipype: A Flexible, Lightweight and Extensible Neuroimaging Data Processing Framework in Python. Front. Neuroinform. 5, 13. https://doi.org/10.3389/fninf.2011.00013

Gorgolewski, K.J., Esteban, O., Ellis, D.G., Notter, M.P., Ziegler, E., Johnson, H., Hamalainen, C., Yvernault, B., Burns, C., Manhães-Savio, A., Jarecka, D., Markiewicz, C.J., Salo, T., Clark, D., Waskom, M., Wong, J., Modat, M., Dewey, B.E., Clark, M.G., Dayan, M., Loney, F., Madison, C., Gramfort, A., Keshavan, A., Berleant, S., Pinsard, B., Goncalves, M., Clark, D., Cipollini, B., Varoquaux, G., Wassermann, D., Rokem, A., Halchenko, Y.O., Forbes, J., Moloney, B., Malone, I.B., Hanke, M., Mordom, D., Buchanan, C., Pauli, W.M., Huntenburg, J.M., Horea, C., Schwartz, Y., Tungaraza, R., Iqbal, S., Kleesiek, J., Sikka, S., Frohlich, C., Kent, J., Perez-Guevara, M., Watanabe, A., Welch, D., Cumba, C., Ginsburg, D., Eshaghi, A., Kastman, E., Bougacha, S., Blair, R., Acland, B., Gillman, A., Schaefer, A., Nichols, B.N., Giavasis, S., Erickson, D., Correa, C., Ghayoor, A., Küttner, R., Haselgrove, C., Zhou, D., Craddock, R.C., Haehn, D., Lampe, L., Millman, J., Lai, J., Renfro, M., Liu, S., Stadler, J., Glatard, T., Kahn, A.E., Kong, X.-Z., Triplett, W., Park, A., McDermottroe, C., Hallquist, M., Poldrack, R.A., Perkins, L.N., Noel, M., Gerhard, S., Salvatore, J., Mertz, F., Broderick, W., Inati, S., Hinds, O., Brett, M., Durnez, J., Tambini, A., Rothmei, S., Andberg, S.K., Cooper, G., Marina, A., Mattfeld, A., Urchs, S., Sharp, P., Matsubara, K., Geisler, D., Cheung, B., Floren, A., Nickson, T., Pannetier, N., Weinstein, A., Dubois, M., Arias, J., Tarbert, C., Schlamp, K., Jordan, K., Liem, F., Saase, V., Harms, R., Khanuja, R., Podranski, K., Flandin, G., Papadopoulos Orfanos, D., Schwabacher, I., McNamee, D., Falkiewicz, M., Pellman, J., Linkersdörfer, J., Varada, J., Pérez-García, F., Davison, A., Shachnev, D., Ghosh, S., 2017. Nipype: a flexible, lightweight and extensible neuroimaging data processing framework in Python. 0.13.1. https://doi.org/10.5281/ZENODO.581704

Greve, D.N., Fischl, B., 2009. Accurate and robust brain image alignment using boundary-based registration. Neuroimage 48, 63–72. https://doi.org/10.1016/j.neuroimage.2009.06.060

Guo, J.Y., Niendam, T.A., Auther, A.M., Carrión, R.E., Cornblatt, B.A., Ragland, J.D., Adelsheim, S., Calkins, R., Sale, T.G., Taylor, S.F., McFarlane, W.R., Carter, C.S., 2019. Predicting psychosis risk using a specific measure of cognitive control: a 12-month longitudinal study. Psychol. Med. 1–10. https://doi.org/10.1017/S0033291719002332

Gur, R.E., Cowell, P.E., Latshaw, A., Turetsky, B.I., Grossman, R.I., Arnold, S.E., Bilker, W.B., Gur, R.C., 2000. Reduced dorsal and orbital prefrontal gray matter volumes in schizophrenia. Arch. Gen. Psychiatry 57, 761–768.

Haroun, N., Dunn, L., Haroun, A., Cadenhead, K.S., 2006. Risk and protection in prodromal schizophrenia: ethical implications for clinical practice and future research. Schizophr. Bull. 32, 166–178. https://doi.org/10.1093/schbul/sbj007

Harris, J.M., Whalley, H., Yates, S., Miller, P., Johnstone, E.C., Lawrie, S.M., 2004. Abnormal cortical folding in high-risk individuals: A predictor of the development of schizophrenia? Biol. Psychiatry 56, 182–189. https://doi.org/10.1016/j.biopsych.2004.04.007

Holzer, L., Urben, S., Passini, C.M., Jaugey, L., Herzog, M.H., Halfon, O., Pihet, S., 2014. A randomized controlled trial of the effectiveness of computer-assisted cognitive remediation (CACR) in adolescents with psychosis or at high risk of psychosis. Behav. Cogn. Psychother. 42, 421–434. https://doi.org/10.1017/S1352465813000313

Hooker, C.I., Carol, E.E., Eisenstein, T.J., Yin, H., Lincoln, S.H., Tully, L.M., Dodell-Feder, D., Nahum, M., Keshavan, M.S., Seidman, L.J., 2014. A pilot study of cognitive training in clinical high risk for psychosis: initial evidence of cognitive benefit. Schizophr. Res. 157, 314–316. https://doi.org/10.1016/j.schres.2014.05.034

Jenkinson, M., Bannister, P., Brady, M., Smith, S.M., 2002. Improved Optimization for the Robust and Accurate Linear Registration and Motion Correction of Brain Images. Neuroimage 17, 825–841. https://doi.org/10.1006/nimg.2002.1132

medRxiv preprint doi: https://doi.org/10.1101/2020.01.20.20018069; this version posted January 27, 2020. The copyright holder has placed this preprint (which was not certified by peer review) in the Public Domain. It is no longer restricted by copyright. Anyone can legally share, reuse, remix, or adapt this material for any purpose without crediting the original authors.

Kim, C., Cilles, S.E., Johnson, N.F., Gold, B.T., 2012. Domain general and domain preferential brain regions associated with different types of task switching: A Meta-Analysis. Hum. Brain Mapp. 33, 130–142. https://doi.org/10.1002/hbm.21199

Koechlin, E., Ody, C., Kouneiher, F., 2003. The architecture of cognitive control in the human prefrontal cortex. Science 302, 1181–1185. https://doi.org/10.1126/science.1088545

Koechlin, E., Summerfield, C., 2007. An information theoretical approach to prefrontal executive function. Trends Cogn. Sci. 11, 229–235. https://doi.org/10.1016/j.tics.2007.04.005

Lesh, T.A., Westphal, A.J., Niendam, T.A., Yoon, J.H., Minzenberg, M.J., Ragland, J.D., Solomon, M., Carter, C.S., 2013. Proactive and reactive cognitive control and dorsolateral prefrontal cortex dysfunction in first episode schizophrenia. Neuroimage Clin 2, 590–599. https://doi.org/10.1016/j.nicl.2013.04.010

MacDonald, A.W., 3rd, Carter, C.S., 2003. Event-related FMRI study of context processing in dorsolateral prefrontal cortex of patients with schizophrenia. J. Abnorm. Psychol. 112, 689–697. https://doi.org/10.1037/0021-843X.112.4.689

MacDonald, A.W., 3rd, Carter, C.S., Kerns, J.G., Ursu, S., Barch, D.M., Holmes, A.J., Stenger, V.A., Cohen, J.D., 2005. Specificity of prefrontal dysfunction and context processing deficits to schizophrenia in never-medicated patients with first-episode psychosis. Am. J. Psychiatry 162, 475–484. https://doi.org/10.1176/appi.ajp.162.3.475

Mann, C.L., Footer, O., Chung, Y.S., Driscoll, L.L., Barch, D.M., 2013. Spared and impaired aspects of motivated cognitive control in schizophrenia. J. Abnorm. Psychol. 122, 745–755. https://doi.org/10.1037/a0033069

McGlashan, T.H., Addington, J., Cannon, T., 2007. Recruitment and treatment practices for help-seeking "prodromal" patients. Schizophrenia.

McGlashan, T.H., Miller, T.J., Woods, S.W., 2001. Pre-onset detection and intervention research in schizophrenia psychoses: current estimates of benefit and risk. Schizophr. Bull. 27, 563–570. https://doi.org/10.1093/oxfordjournals.schbul.a006896

McGlashan, T.H., Zipursky, R.B., Perkins, D., Addington, J., Miller, T.J., Woods, S.W., Hawkins, K.A., Hoffman, R., Lindborg, S., Tohen, M., Breier, A., 2003. The PRIME North America randomized double-blind clinical trial of olanzapine versus placebo in patients at risk of being prodromally symptomatic for psychosis. I. Study rationale and design. Schizophr. Res. 61, 7–18.

Miller, E.K., Cohen, J.D., 2001. An integrative theory of prefrontal cortex function. Annu. Rev. Neurosci. 24, 167–202. https://doi.org/10.1146/annurev.neuro.24.1.167

Miller, T.J., Mcglashan, T.H., Woods, S.W., Stein, K., Driesen, N., Corcoran, C.M., Hoffman, R., Davidson, L., 1999. Symptom assessment in schizophrenic prodromal states. Psychiatr. Q. 70, 273–287.

Minzenberg, M.J., Laird, A.R., Thelen, S., Carter, C.S., Glahn, D.C., 2009. Meta-analysis of 41 functional neuroimaging studies of executive function in schizophrenia. Arch. Gen. Psychiatry 66, 811–822. https://doi.org/10.1001/archgenpsychiatry.2009.91

Monsell, S., 1996. Control of mental processes. Unsolved mysteries of the mind: Tutorial essays in cognition 93–148.

Morey, R.A., Inan, S., Mitchell, T.V., Perkins, D.O., Lieberman, J.A., Belger, A., 2005. Imaging frontostriatal function in ultra-high-risk, early, and chronic schizophrenia during executive processing. Arch. Gen. Psychiatry 62, 254–262. https://doi.org/10.1001/archpsyc.62.3.254

Morrison, A.P., French, P., Stewart, S.L.K., Birchwood, M., Fowler, D., Gumley, A.I., Jones, P.B., Bentall, R.P., Lewis, S.W., Murray, G.K., Patterson, P., Brunet, K., Conroy, J., Parker, S., Reilly, T., Byrne, R., Davies, L.M., Dunn, G., 2012. Early detection and intervention evaluation for people at risk of psychosis: multisite randomised controlled trial. BMJ 344, e2233. https://doi.org/10.1136/bmj.e2233

Morrison, A.P., French, P., Walford, L., Lewis, S.W., Kilcommons, A., Green, J., Parker, S., Bentall, R.P., 2004. Cognitive therapy for the prevention of psychosis in people at ultra-high risk: randomised controlled trial. Br. J. Psychiatry 185, 291–297. https://doi.org/10.1192/bjp.185.4.291

medRxiv preprint doi: https://doi.org/10.1101/2020.01.20.20018069; this version posted January 27, 2020. The copyright holder has placed this preprint (which was not certified by peer review) in the Public Domain. It is no longer restricted by copyright. Anyone can legally share, reuse, remix, or adapt this material for any purpose without crediting the original authors.

Nee, D.E., D'Esposito, M., 2016. The hierarchical organization of the lateral prefrontal cortex. Elife 5, 1–26. https://doi.org/10.7554/eLife.12112

Niendam, T.A., Lesh, T.A., Yoon, J., Westphal, A.J., Hutchinson, N., Ragland, J.D., Solomon, M., Minzenberg, M., Carter, C.S., 2014. Impaired context processing as a potential marker of psychosis risk state | Kopernio. Psychiatry Res. 221, 13–20. https://doi.org/10.1016/j.pscychresns.2013.09.001

Oh, J.S., Kubicki, M., Rosenberger, G., Bouix, S., Levitt, J.J., McCarley, R.W., Westin, C.-F., Shenton, M.E., 2009. Thalamo-frontal white matter alterations in chronic schizophrenia: a quantitative diffusion tractography study. Hum. Brain Mapp. 30, 3812–3825. https://doi.org/10.1002/hbm.20809

Pantelis, C., Wannan, C., Bartholomeusz, C.F., Allott, K., McGorry, P.D., 2015. Cognitive intervention in early psychosis — preserving abilities versus remediating deficits. Current Opinion in Behavioral Sciences. https://doi.org/10.1016/j.cobeha.2015.02.008

Pelletier-Baldelli, A., Orr, J.M., Bernard, J.A., Mittal, V.A., 2018. Social reward processing: A biomarker for predicting psychosis risk? Schizophr. Res. https://doi.org/10.1016/j.schres.2018.07.042

Pettersson-Yeo, W., Allen, P., Benetti, S., McGuire, P., Mechelli, A., 2011. Dysconnectivity in schizophrenia: where are we now? Neurosci. Biobehav. Rev. 35, 1110–1124. https://doi.org/10.1016/j.neubiorev.2010.11.004

Poppe, A.B., Barch, D.M., Carter, C.S., Gold, J.M., Ragland, J.D., Silverstein, S.M., MacDonald, A.W., 2016. Reduced Frontoparietal Activity in Schizophrenia Is Linked to a Specific Deficit in Goal Maintenance: A Multisite Functional Imaging Study. Schizophr. Bull. 1–9. https://doi.org/10.1093/schbul/sbw036

Preti, A., Cella, M., 2010. Randomized-controlled trials in people at ultra high risk of psychosis: a review of treatment effectiveness. Schizophr. Res. 123, 30–36. https://doi.org/10.1016/j.schres.2010.07.026

Pruim, R.H.R., Mennes, M., van Rooij, D., Llera, A., Buitelaar, J.K., Beckmann, C.F., 2015. ICA-AROMA: A robust ICA-based strategy for removing motion artifacts from fMRI data. Neuroimage 112, 267–277. https://doi.org/10.1016/j.neuroimage.2015.02.064

Ragland, J.D., Blumenfeld, R.S., Ramsay, I.S., Yonelinas, A., Yoon, J., Solomon, M., Carter, C.S., Ranganath, C., 2012. Neural correlates of relational and item-specific encoding during working and long-term memory in schizophrenia. Neuroimage 59, 1719–1726. https://doi.org/10.1016/j.neuroimage.2011.08.055

Repovs, G., Csernansky, J.G., Barch, D.M., 2011. Brain network connectivity in individuals with schizophrenia and their siblings. Biol. Psychiatry 69, 967–973. https://doi.org/10.1016/j.biopsych.2010.11.009

Robinson, E.C., Garcia, K., Glasser, M.F., Chen, Z., Coalson, T.S., Makropoulos, A., Bozek, J., Wright, R., Schuh, A., Webster, M., Hutter, J., Price, A., Cordero Grande, L., Hughes, E., Tusor, N., Bayly, P.V., Van Essen, D.C., Smith, S.M., Edwards, A.D., Hajnal, J., Jenkinson, M., Glocker, B., Rueckert, D., 2018. Multimodal surface matching with higher-order smoothness constraints. Neuroimage 167, 453–465. https://doi.org/10.1016/j.neuroimage.2017.10.037

Robinson, E.C., Jbabdi, S., Glasser, M.F., Andersson, J., Burgess, G.C., Harms, M.P., Smith, S.M., Van Essen, D.C., Jenkinson, M., 2014. MSM: a new flexible framework for Multimodal Surface Matching. Neuroimage 100, 414–426. https://doi.org/10.1016/j.neuroimage.2014.05.069

Rotarska-Jagiela, A., van de Ven, V., Oertel-Knöchel, V., Uhlhaas, P.J., Vogeley, K., Linden, D.E.J., 2010. Resting-state functional network correlates of psychotic symptoms in schizophrenia. Schizophr. Res. 117, 21–30. https://doi.org/10.1016/j.schres.2010.01.001

Ruge, H., Jamadar, S., Zimmermann, U., Karayanidis, F., 2013. The many faces of preparatory control in task switching: reviewing a decade of fMRI research. Hum. Brain Mapp. 34, 12–35. https://doi.org/10.1002/hbm.21420

Sallet, P.C., Elkis, H., Alves, T.M., Oliveira, J.R., Sassi, E., Campi de Castro, C., Busatto, G.F., Gattaz, W.F., 2003. Reduced cortical folding in schizophrenia: an MRI morphometric study. Am. J. Psychiatry 160, 1606–1613. https://doi.org/10.1176/appi.ajp.160.9.1606

medRxiv preprint doi: https://doi.org/10.1101/2020.01.20.20018069; this version posted January 27, 2020. The copyright holder has placed this preprint (which was not certified by peer review) in the Public Domain. It is no longer restricted by copyright. Anyone can legally share, reuse, remix, or adapt this material for any purpose without crediting the original authors.

Seidman, L.J., Thermenos, H.W., Poldrack, R.A., Peace, N.K., Koch, J.K., Faraone, S.V., Tsuang, M.T., 2006. Altered brain activation in dorsolateral prefrontal cortex in adolescents and young adults at genetic risk for schizophrenia: an fMRI study of working memory. Schizophr. Res. 85, 58–72. https://doi.org/10.1016/j.schres.2006.03.019

Sheffield, J.M., Gold, J.M., Strauss, M.E., Carter, C.S., MacDonald, A.W., Ragland, J.D., Silverstein, S.M., Barch, D.M., 2014. Common and specific cognitive deficits in schizophrenia: relationships to function. Cogn. Affect. Behav. Neurosci. 14, 161–174. https://doi.org/10.3758/s13415-013-0211-5

Smith, S.M., Jenkinson, M., Woolrich, M.W., Beckmann, C.F., Behrens, T.E.J., Johansen-Berg, H., Bannister, P.R., De Luca, M., Drobnjak, I., Flitney, D.E., Niazy, R.K., Saunders, J., Vickers, J., Zhang, Y., De Stefano, N., Brady, J.M., Matthews, P.M., 2004. Advances in functional and structural MR image analysis and implementation as FSL. Neuroimage 23 Suppl 1, S208–S219. https://doi.org/10.1016/j.neuroimage.2004.07.051

Stanfield, A.C., Moorhead, T.W.J., Harris, J.M., Owens, D.G.C., Lawrie, S.M., Johnstone, E.C., 2008. Increased Right Prefrontal Cortical Folding in Adolescents at Risk of Schizophrenia for Cognitive Reasons. Biol. Psychiatry 63, 80–85. https://doi.org/10.1016/j.biopsych.2007.04.012

Stuss, D.T., Alexander, M.P., 2000. Executive functions and the frontal lobes: a conceptual view. Psychol. Res. 63, 289–298. https://doi.org/10.1007/s004269900007

The jamovi project, 2019. jamovi.

Thompson, E., Millman, Z.B., Okuzawa, N., Mittal, V., DeVylder, J., Skadberg, T., Buchanan, R.W., Reeves, G.M., Schiffman, J., 2015. Evidence-based early interventions for individuals at clinical high risk for psychosis: a review of treatment components. J. Nerv. Ment. Dis. 203, 342–351. https://doi.org/10.1097/NMD.0000000000000287

Tustison, N.J., Avants, B.B., Cook, P.A., Yuanjie Zheng, Egan, A., Yushkevich, P.A., Gee, J.C., 2010. N4ITK: Improved N3 Bias Correction. IEEE Trans. Med. Imaging 29, 1310–1320. https://doi.org/10.1109/TMI.2010.2046908

van den Heuvel, M.P., Mandl, R.C.W., Stam, C.J., Kahn, R.S., Pol, H.E.H., 2010. Aberrant Frontal and Temporal Complex Network Structure in Schizophrenia: A Graph Theoretical Analysis. Journal of Neuroscience 30, 15915–15926. https://doi.org/10.1523/JNEUROSCI.2874-10.2010

White, T., Anjum, A., Schulz, S.C., 2006. The schizophrenia prodrome. Am. J. Psychiatry 163, 376–380. https://doi.org/10.1176/appi.ajp.163.3.376

Winkler, A.M., Ridgway, G.R., Webster, M.A., Smith, S.M., Nichols, T.E., 2014. Permutation inference for the general linear model. Neuroimage 92, 381–397. https://doi.org/10.1016/j.neuroimage.2014.01.060

Woods, S.W., Tully, E.M., Walsh, B.C., Hawkins, K.A., Callahan, J.L., Cohen, S.J., Mathalon, D.H., Miller, T.J., McGlashan, T.H., 2007. Aripiprazole in the treatment of the psychosis prodrome: an open-label pilot study. Br. J. Psychiatry 191, s96–s101.

Woods, S.W., Walsh, B.C., Addington, J., Cadenhead, K.S., Cannon, T.D., Cornblatt, B.A., Heinssen, R., Perkins, D.O., Seidman, L.J., Tarbox, S.I., Tsuang, M.T., Walker, E.F., McGlashan, T.H., 2014. Current status specifiers for patients at clinical high risk for psychosis. Schizophr. Res. 158, 69–75. https://doi.org/10.1016/j.schres.2014.06.022

Woods, S.W., Walsh, B.C., Hawkins, K.A., Miller, T.J., Saksa, J.R., D'Souza, D.C., Pearlson, G.D., Javitt, D.C., McGlashan, T.H., Krystal, J.H., 2013. Glycine treatment of the risk syndrome for psychosis: report of two pilot studies. Eur. Neuropsychopharmacol. 23, 931–940. https://doi.org/10.1016/j.euroneuro.2012.09.008

Woolgar, A., Hampshire, A., Thompson, R., Duncan, J., 2011. Adaptive coding of task-relevant information in human frontoparietal cortex. Journal of Neuroscience 31, 14592–14599. https://doi.org/10.1523/JNEUROSCI.2616-11.2011

Woolrich, M.W., Ripley, B.D., Brady, M., Smith, S.M., 2001. Temporal Autocorrelation in Univariate Linear Modeling of FMRI Data. Neuroimage 14, 1370–1386. https://doi.org/10.1006/nimg.2001.0931

medRxiv preprint doi: https://doi.org/10.1101/2020.01.20.20018069; this version posted January 27, 2020. The copyright holder has placed this preprint (which was not certified by peer review) in the Public Domain. It is no longer restricted by copyright. Anyone can legally share, reuse, remix, or adapt this material for any purpose without crediting the original authors.

Yung, A.R., McGorry, P.D., 1996. The prodromal phase of first-episode psychosis: past and current conceptualizations. Schizophr. Bull. 22, 353–370. https://doi.org/10.1093/schbul/22.2.353

Yung, A.R., Yuen, H.P., Berger, G., Francey, S., Hung, T.-C., Nelson, B., Phillips, L., McGorry, P., 2007. Declining transition rate in ultra high risk (prodromal) services: dilution or reduction of risk? Schizophr. Bull. 33, 673–681. https://doi.org/10.1093/schbul/sbm015

Zhang, Y., Brady, M., Smith, S., 2001. Segmentation of brain MR images through a hidden Markov random field model and the expectation-maximization algorithm. IEEE Trans. Med. Imaging 20, 45–57. https://doi.org/10.1109/42.906424

Zhou, Y., Liang, M., Jiang, T., Tian, L., Liu, Y., Liu, Z., Liu, H., Kuang, F., 2007. Functional dysconnectivity of the dorsolateral prefrontal cortex in first-episode schizophrenia using resting-state fMRI. Neurosci. Lett. 417, 297–302. https://doi.org/10.1016/j.neulet.2007.02.081

medRxiv preprint doi: https://doi.org/10.1101/2020.01.20.20018069; this version posted January 27, 2020. The copyright holder has placed this preprint (which was not certified by peer review) in the Public Domain. It is no longer restricted by copyright. Anyone can legally share, reuse, remix, or adapt this material for any purpose without crediting the original authors.

Figure Legends

Figure 1. Example task block. At the beginning of a block three instruction cues were presented that defined the current task. Each cue was presented one at a time in the following order: logic cue, semantic cue, response cue. There were 4 possible logic cues, 4 possible semantic cues, and 4 possible response cues, yielding 64 possible tasks from all combinations. Of the 64 possible tasks, 4 were practiced before scanning and the remainder were only shown once each in a scanning session. Participants then performed three trials of the task, indicating if the current task rule was true or false.

Figure 2. Activation during novel and practiced tasks at task cue encoding and task performance. Results were corrected at the parcel level with permutation testing to a threshold of $-\log(p) > 1.778$ (equivalent to $p<.05$ with Bonferroni correction for 3 tests: Left Cortical Surface, Right Cortical Surface, subcortical dense volume). Outlines depict the areal boundaries of the Glasser et al. HCP Multi-modal Parcellation [91], and labels come from that parcellation. Novel trial activation is shown in red, practiced task activation is shown in blue, and overlapping activation is shown in purple. Lateral and medial cortical surfaces of both hemispheres are shown in Supplemental Figure 1, and subcortical volumes are shown in Supplemental Figure 2.

Figure 3. Effect size maps of contrasts of novel and practiced tasks at task cue encoding and task performance. Outlines depict the areal boundaries of the Glasser et al. HCP Multi-modal Parcellation [91], and labels come from that parcellation. The contrast of Novel > Practiced is

medRxiv preprint doi: https://doi.org/10.1101/2020.01.20.20018069; this version posted January 27, 2020. The copyright holder has placed this preprint (which was not certified by peer review) in the Public Domain. It is no longer restricted by copyright. Anyone can legally share, reuse, remix, or adapt this material for any purpose without crediting the original authors.

shown in hot colors and the contrast of Practiced > Novel is shown in cold colors. Values shown are Cohen's D with a minimum threshold of 0.3. Lateral and medial cortical surfaces of both hemispheres are shown in Supplemental Figure 3 and subcortical volumes are shown in Supplemental Figure 4.

Figure 4. Effect size maps of contrasts of the Healthy Control (HC) group and the Clinical High Risk (CHR) group for novel and practiced tasks at task cue encoding and task performance. Outlines depict the areal boundaries of the Glasser et al. HCP Multi-modal Parcellation [91], and labels come from that parcellation. The contrast of HC > CHR is shown in hot colors and the contrast of CHR > HC is shown in cold colors. Values shown are Cohen's D with a minimum threshold of 0.3. Lateral and medial cortical surfaces of both hemispheres are shown in Supplemental Figure 5, and subcortical volumes are shown in Supplemental Figure 6.

Supplemental Figure 1. Full cortical surface results of the analysis of activation during novel and practiced tasks at task cue encoding and task performance shown in Figure 1. Results are corrected at the parcel level with permutation testing to a threshold of -log(p) > 1.778, which is equivalent to p<.05 with Bonferroni correction for 3 tests: Left Cortical Surface, Right Cortical Surface, subcortical volume. Outlines depict the areal boundaries of the Glasser et al. HCP Multi-modal Parcellation [91], and labels come from that parcellation. Novel trial activation is shown in red, Practiced task activation is shown in blue, and overlapping activation is shown in purple.

Supplemental Figure 2. Full subcortical volume results of the analysis of activation during novel and

medRxiv preprint doi: https://doi.org/10.1101/2020.01.20.20018069; this version posted January 27, 2020. The copyright holder has placed this preprint (which was not certified by peer review) in the Public Domain. It is no longer restricted by copyright. Anyone can legally share, reuse, remix, or adapt this material for any purpose without crediting the original authors.

practiced tasks at task cue encoding and task performance shown in Figure 1. Results were corrected using Threshold-Free Cluster Enhancement with permutation testing to a threshold of -log(p) > 1.778, which is equivalent to p<.05 with Bonferroni correction for 3 tests: Left Cortical Surface, Right Cortical Surface, subcortical volume. A cluster extent of 15 contiguous voxels was also applied. Novel trial activation is shown in red, practiced task activation is shown in blue, and overlapping activation is shown in purple.

Supplemental Figure 3. Effect size maps of contrasts of novel and practiced tasks at task cue encoding and task performance displayed on the lateral and medial cortical surfaces of both hemispheres (full set of results shown in Figure 3). Outlines depict the areal boundaries of the Glasser et al. HCP Multi-modal Parcellation [91], and labels come from that parcellation. The contrast of Novel > Practiced is shown in hot colors and the contrast of Practiced > Novel is shown in cold colors. Values shown are Cohen's D with a minimum threshold of 0.3.

Supplemental Figure 4. Effect size maps of contrasts of novel and practiced tasks at task cue encoding and task performance displayed on the subcortical volumes (full set of results shown in Figure 3). Y-coordinate of each slice is depicted in the lower right corner of each slice. The contrast of Novel > Practiced is shown in hot colors and the contrast of Practiced > Novel is shown in cold colors. Values shown are Cohen's D with a minimum threshold of 0.3.

Supplemental Figure 5. Effect size maps of contrasts of the Healthy Control (HC) group and the Clinical High Risk (CHR) group for novel and practiced tasks at task cue encoding and task

medRxiv preprint doi: https://doi.org/10.1101/2020.01.20.20018069; this version posted January 27, 2020. The copyright holder has placed this preprint (which was not certified by peer review) in the Public Domain. It is no longer restricted by copyright. Anyone can legally share, reuse, remix, or adapt this material for any purpose without crediting the original authors.

performance displayed on the lateral and medial cortical surfaces of both hemispheres (full set of results shown in Figure 4). Outlines depict the areal boundaries of the Glasser et al. HCP Multi-modal Parcellation [91], and labels come from that parcellation. The contrast of Novel > Practiced is shown in hot colors and the contrast of Practiced > Novel is shown in cold colors. Values shown are Cohen's D with a minimum threshold of 0.3.

Supplemental Figure 6. Effect size maps of contrasts of the Healthy Control (HC) group and the Clinical High Risk (CHR) group for novel and practiced tasks at task cue encoding and task performance displayed on the subcortical volumes (full set of results shown in Figure 4). Y-coordinate of each slice is depicted in the lower right corner of each slice. The contrast of Novel > Practiced is shown in hot colors and the contrast of Practiced > Novel is shown in cold colors. Values shown are Cohen's D with a minimum threshold of 0.3.

medRxiv preprint doi: https://doi.org/10.1101/2020.01.20.20018069; this version posted January 27, 2020. The copyright holder has placed this preprint (which was not certified by peer review) in the Public Domain. It is no longer restricted by copyright. Anyone can legally share, reuse, remix, or adapt this material for any purpose without crediting the original authors.

Tables

Table 1. Symptoms and demographics

	CHR *M(SEM)*	**HC *M(SEM)***	**Statistic**	***p***
Age	20.8(1.54)	21.5(1.83)	t(44) = 2.23	0.05
Education (years)	13.25(0.24)	13.55(0.34)	t(44) = 0.73	0.47
Parent education (years	16.21(0.48)	15.60(0.62)	t(44) = 0.78	0.44
Total positive symptoms (SIPS)	12.23(4.19)	6.35(6.49)	t(44) = 3.52	0.001
Gender	CHR (n)	HC (n)	$\chi 2(1) = 0.83$	0.36
Male	13	14		
Female	9	11		
Total	22	24		

Abbreviations: CHR, clinical high risk; HC, healthy control; SIPS, Structured Interview for Prodromal Syndromes.

medRxiv preprint doi: https://doi.org/10.1101/2020.01.20.20018069; this version posted January 27, 2020. The copyright holder has placed this preprint (which was not certified by peer review) in the Public Domain. It is no longer restricted by copyright. Anyone can legally share, reuse, remix, or adapt this material for any purpose without crediting the original authors.

Table 2. Estimated marginal means for reaction time by task type and block. SE=standard error.

				95% Confidence Interval	
Task Type	**Block**	**Mean**	**SE**	**Lower**	**Upper**
Novel	1	1342	39	1264	1420
	2	1290	39	1212	1368
	3	1270	39	1192	1348
	4	1255	39	1177	1333
	5	1229	39	1151	1307
	6	1210	39	1132	1288
Practiced	1	1289	39	1211	1367
	2	1254	39	1176	1332
	3	1222	39	1145	1300
	4	1204	39	1126	1282
	5	1198	39	1120	1276
	6	1201	39	1124	1279

medRxiv preprint doi: https://doi.org/10.1101/2020.01.20.20018069; this version posted January 27, 2020. The copyright holder has placed this preprint (which was not certified by peer review) in the Public Domain. It is no longer restricted by copyright. Anyone can legally share, reuse, remix, or adapt this material for any purpose without crediting the original authors.

Table 3. Estimated marginal means for accuracy by task type and block. SE=standard error.

				95% Confidence Interval	
Task Type	**Block**	**Mean**	**SE**	**Lower**	**Upper**
Novel	1	77.7%	2.2%	73.4%	82.0%
	2	80.9%	2.2%	76.6%	85.2%
	3	81.8%	2.2%	77.4%	86.1%
	4	82.6%	2.2%	78.3%	86.9%
	5	81.1%	2.2%	76.7%	85.4%
	6	81.3%	2.2%	77.0%	85.7%
Practiced	1	83.5%	2.2%	79.2%	87.8%
	2	86.7%	2.2%	82.4%	91.1%
	3	87.3%	2.2%	82.9%	91.6%
	4	87.7%	2.2%	83.4%	92.0%
	5	84.4%	2.2%	80.0%	88.7%
	6	85.2%	2.2%	80.9%	89.5%

medRxiv preprint doi: https://doi.org/10.1101/2020.01.20.20018069; this version posted January 27, 2020. The copyright holder has placed this preprint (which was not certified by peer review) in the Public Domain. It is no longer restricted by copyright. Anyone can legally share, reuse, remix, or adapt this material for any purpose without crediting the original authors.

Supplemental Figures

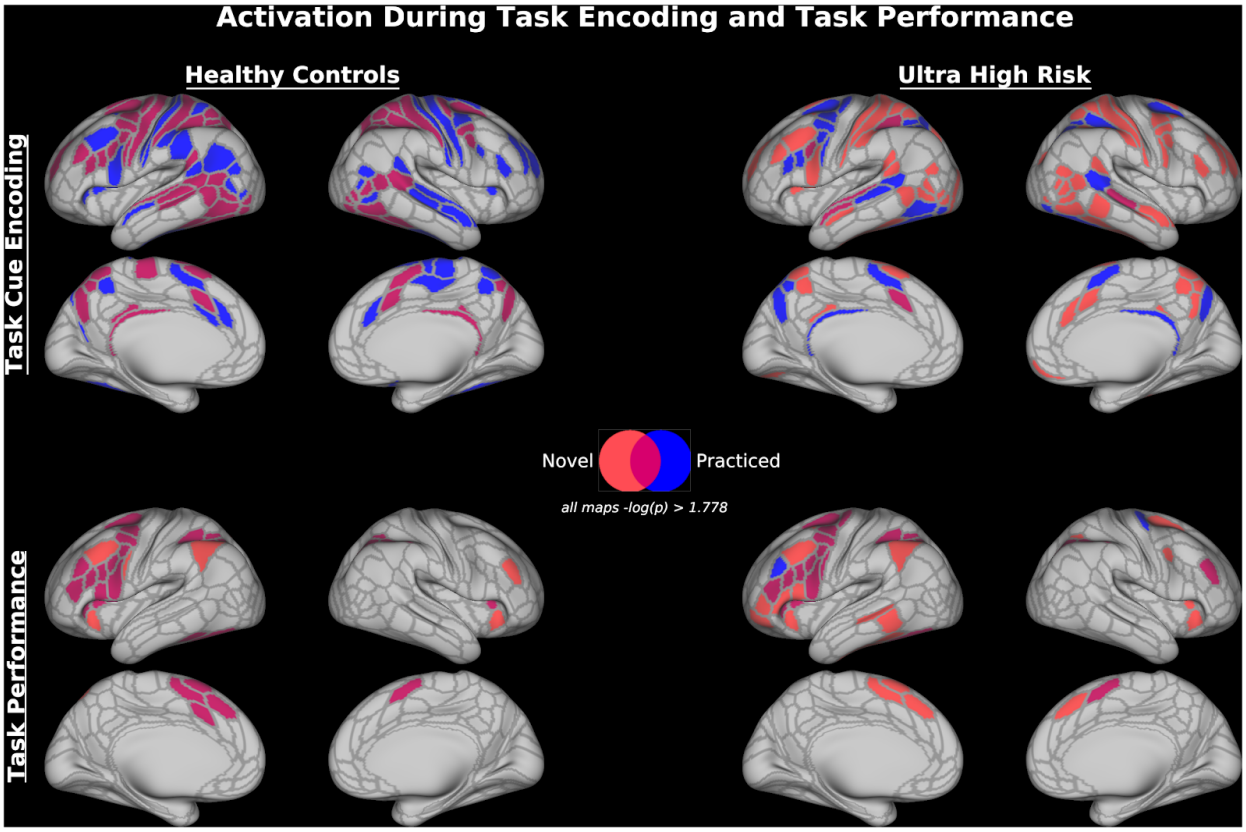

Supplemental Figure 1. Full cortical surface results of the analysis of activation during novel and practiced tasks at task cue encoding and task performance shown in Figure 1. Results are corrected at the parcel level with permutation testing to a threshold of -log(p) > 1.778, which is equivalent to p<.05 with Bonferroni correction for 3 tests: Left Cortical Surface, Right Cortical Surface, subcortical volume. Outlines depict the areal boundaries of the Glasser et al. HCP Multi-modal Parcellation [91], and labels come from that parcellation. Novel trial activation is shown in red, Practiced task activation is shown in blue, and overlapping activation is shown in purple.

medRxiv preprint doi: https://doi.org/10.1101/2020.01.20.20018069; this version posted January 27, 2020. The copyright holder has placed this preprint (which was not certified by peer review) in the Public Domain. It is no longer restricted by copyright. Anyone can legally share, reuse, remix, or adapt this material for any purpose without crediting the original authors.

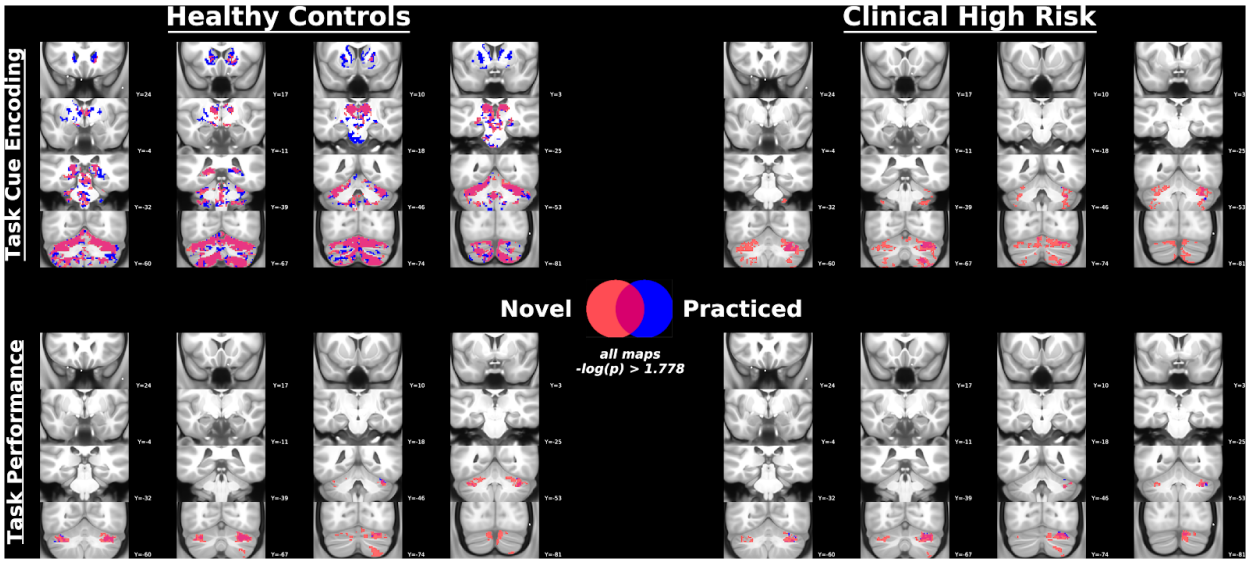

Supplemental Figure 2. Full subcortical volume results of the analysis of activation during novel and practiced tasks at task cue encoding and task performance shown in Figure 1. Results were corrected using Threshold-Free Cluster Enhancement with permutation testing to a threshold of -log(p) > 1.778, which is equivalent to p<.05 with Bonferroni correction for 3 tests: Left Cortical Surface, Right Cortical Surface, subcortical volume. A cluster extent of 15 contiguous voxels was also applied. Novel trial activation is shown in red, practiced task activation is shown in blue, and overlapping activation is shown in purple.

medRxiv preprint doi: https://doi.org/10.1101/2020.01.20.20018069; this version posted January 27, 2020. The copyright holder has placed this preprint (which was not certified by peer review) in the Public Domain. It is no longer restricted by copyright. Anyone can legally share, reuse, remix, or adapt this material for any purpose without crediting the original authors.

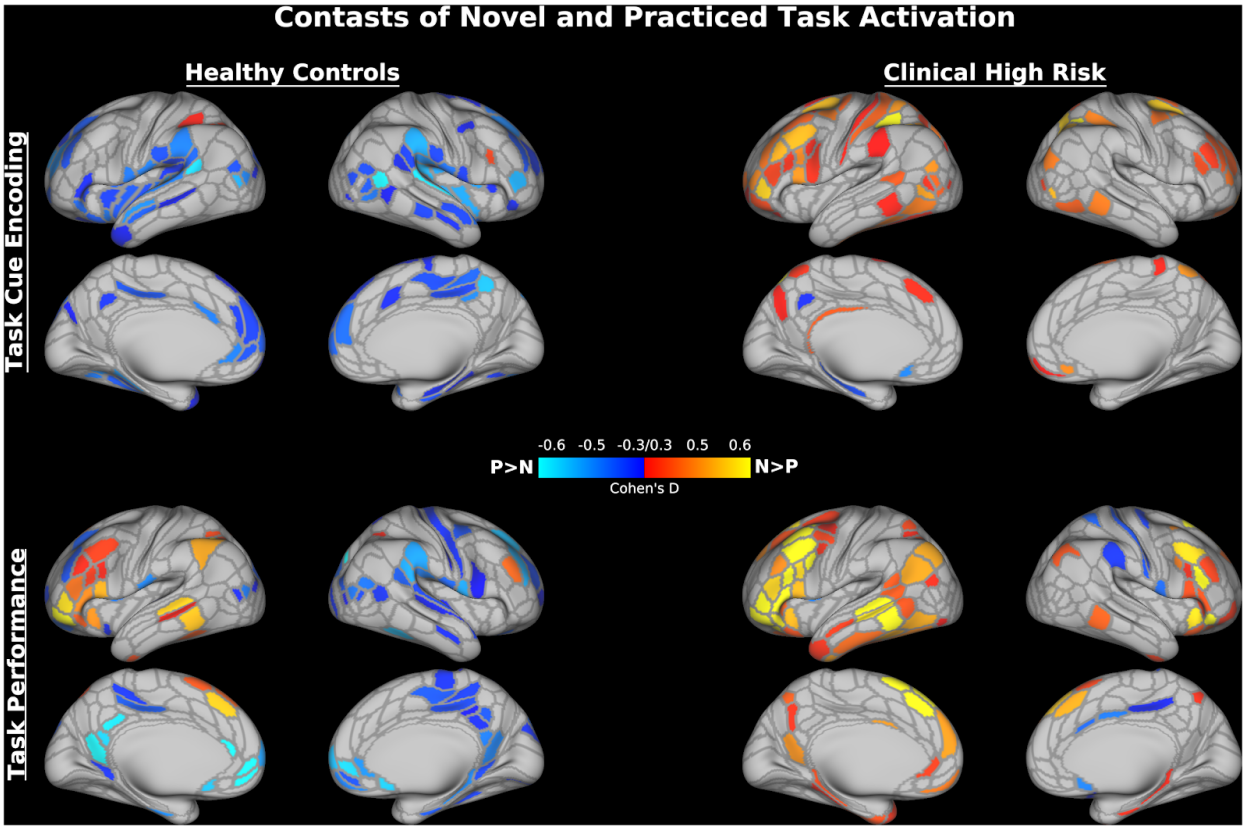

Supplemental Figure 3. Effect size maps of contrasts of novel and practiced tasks at task cue encoding and task performance displayed on the lateral and medial cortical surfaces of both hemispheres (full set of results shown in Figure 3). Outlines depict the areal boundaries of the Glasser et al. HCP Multi-modal Parcellation [91], and labels come from that parcellation. The contrast of Novel > Practiced is shown in hot colors and the contrast of Practiced > Novel is shown in cold colors. Values shown are Cohen's D with a minimum threshold of 0.3.

medRxiv preprint doi: https://doi.org/10.1101/2020.01.20.20018069; this version posted January 27, 2020. The copyright holder has placed this preprint (which was not certified by peer review) in the Public Domain. It is no longer restricted by copyright. Anyone can legally share, reuse, remix, or adapt this material for any purpose without crediting the original authors.

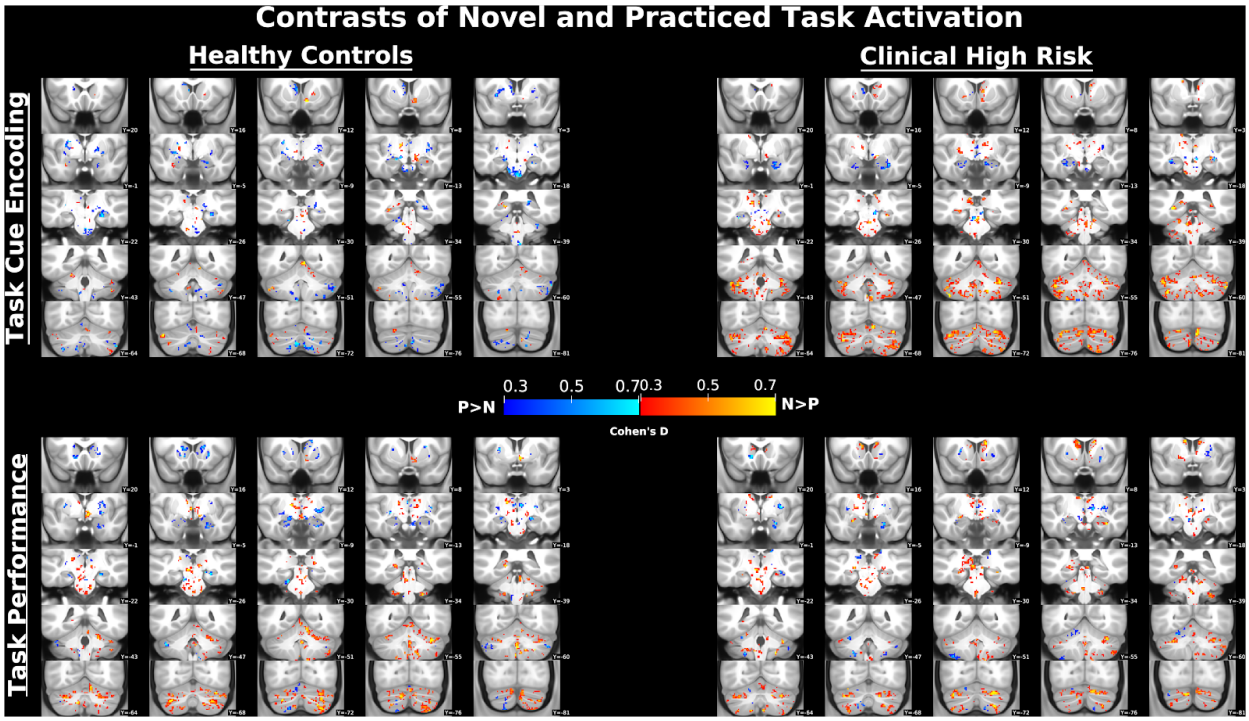

Supplemental Figure 4. Effect size maps of contrasts of novel and practiced tasks at task cue encoding and task performance displayed on the subcortical volumes (full set of results shown in Figure 3). Y-coordinate of each slice is depicted in the lower right corner of each slice. The contrast of Novel > Practiced is shown in hot colors and the contrast of Practiced > Novel is shown in cold colors. Values shown are Cohen's D with a minimum threshold of 0.3.

medRxiv preprint doi: https://doi.org/10.1101/2020.01.20.20018069; this version posted January 27, 2020. The copyright holder has placed this preprint (which was not certified by peer review) in the Public Domain. It is no longer restricted by copyright. Anyone can legally share, reuse, remix, or adapt this material for any purpose without crediting the original authors.

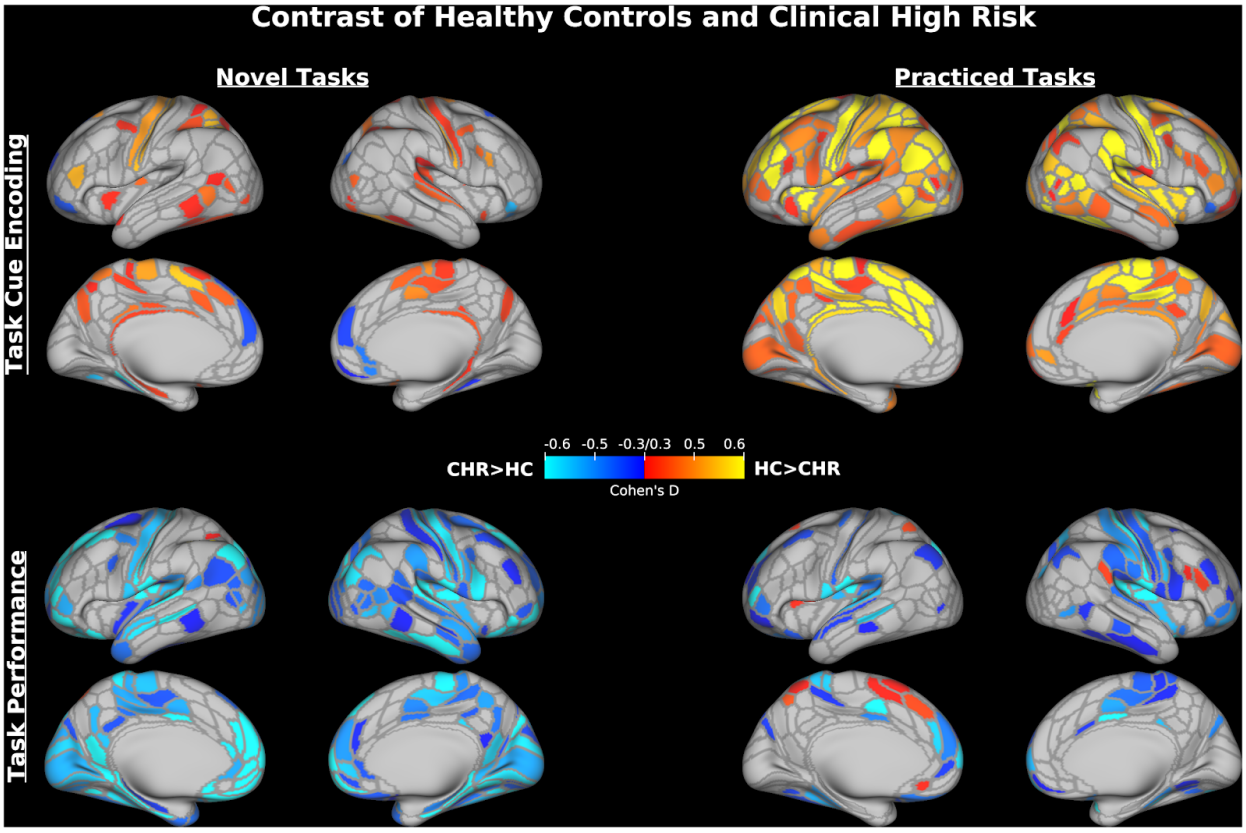

Supplemental Figure 5. Effect size maps of contrasts of the Healthy Control (HC) group and the Clinical High Risk (CHR) group for novel and practiced tasks at task cue encoding and task performance displayed on the lateral and medial cortical surfaces of both hemispheres (full set of results shown in Figure 4). Outlines depict the areal boundaries of the Glasser et al. HCP Multi-modal Parcellation [91], and labels come from that parcellation. The contrast of Novel > Practiced is shown in hot colors and the contrast of Practiced > Novel is shown in cold colors. Values shown are Cohen's D with a minimum threshold of 0.3.

medRxiv preprint doi: https://doi.org/10.1101/2020.01.20.20018069; this version posted January 27, 2020. The copyright holder has placed this preprint (which was not certified by peer review) in the Public Domain. It is no longer restricted by copyright. Anyone can legally share, reuse, remix, or adapt this material for any purpose without crediting the original authors.

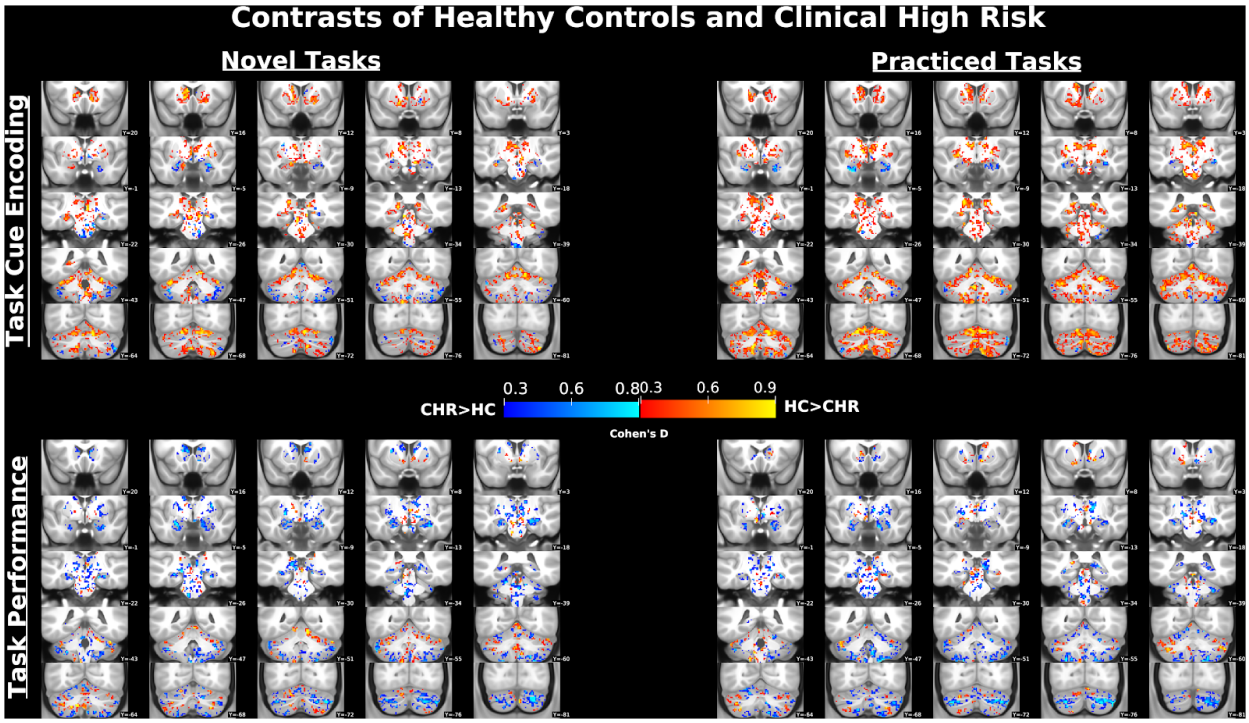

Supplemental Figure 6. Effect size maps of contrasts of the Healthy Control (HC) group and the Clinical High Risk (CHR) group for novel and practiced tasks at task cue encoding and task performance displayed on the subcortical volumes (full set of results shown in Figure 4). Y-coordinate of each slice is depicted in the lower right corner of each slice. The contrast of Novel > Practiced is shown in hot colors and the contrast of Practiced > Novel is shown in cold colors. Values shown are Cohen's D with a minimum threshold of 0.3.

A. **Timeline of 1 block**

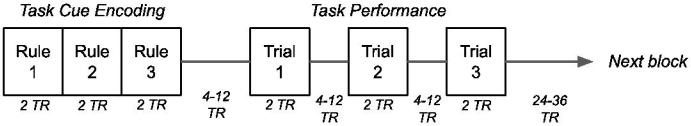

B. **Task Example**

Task: If the answer to the question "Is it sweet?" is the same for both trial words, press the left index key (else press left middle key)

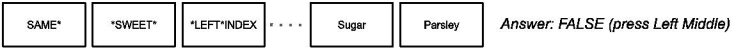

Task cues

1. Logic Cue: SAME, JUST ONE, SECOND, NOT SECOND
2. Semantic Cue: SWEET, LOUD, SOFT, GREEN
3. Response Cue: LEFT INDEX, LEFT MIDDLE, RIGHT INDEX, RIGHT MIDDLE

Activation During Task Encoding and Task Performance

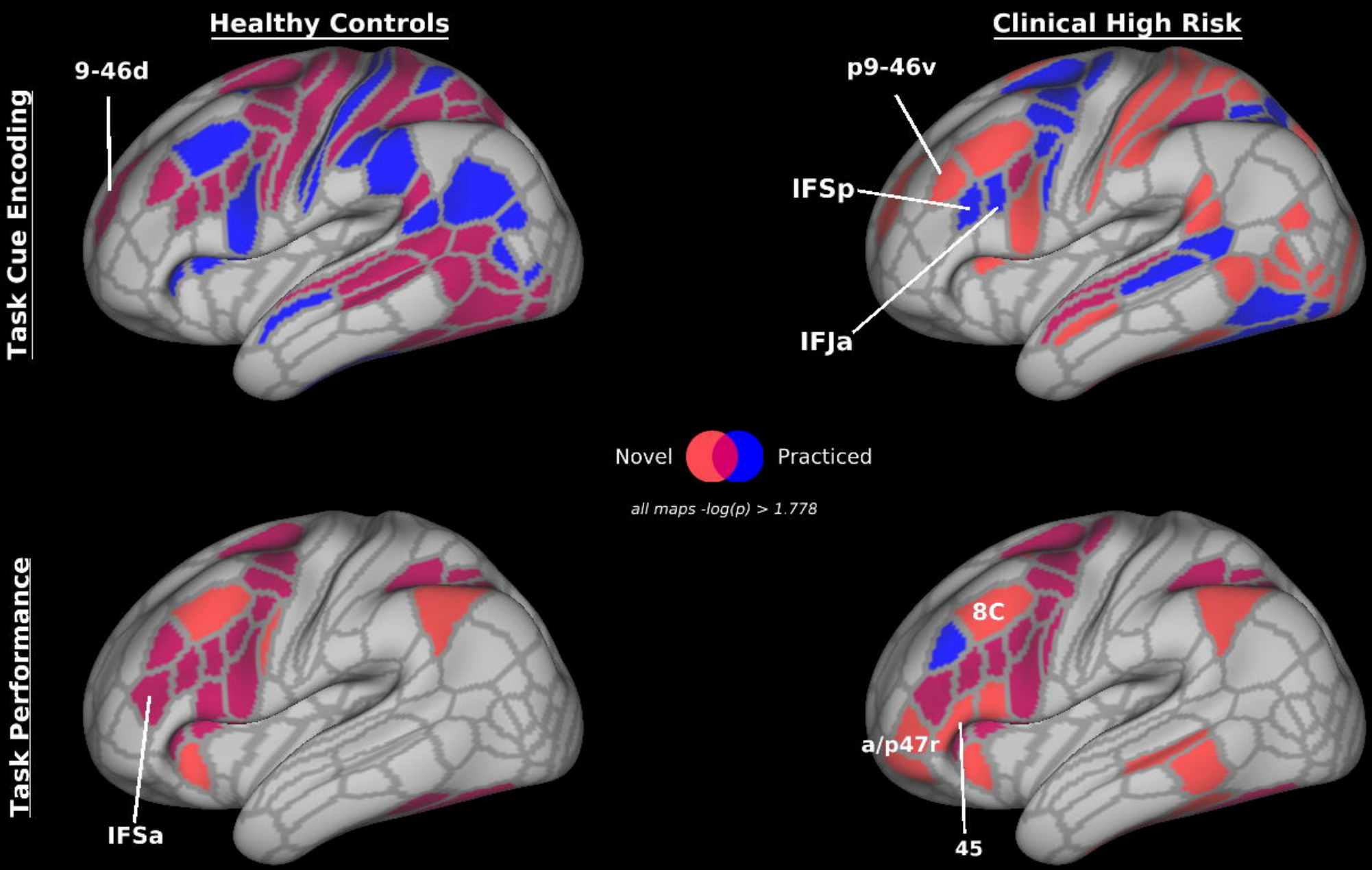

Contasts of Novel and Practiced Task Activation

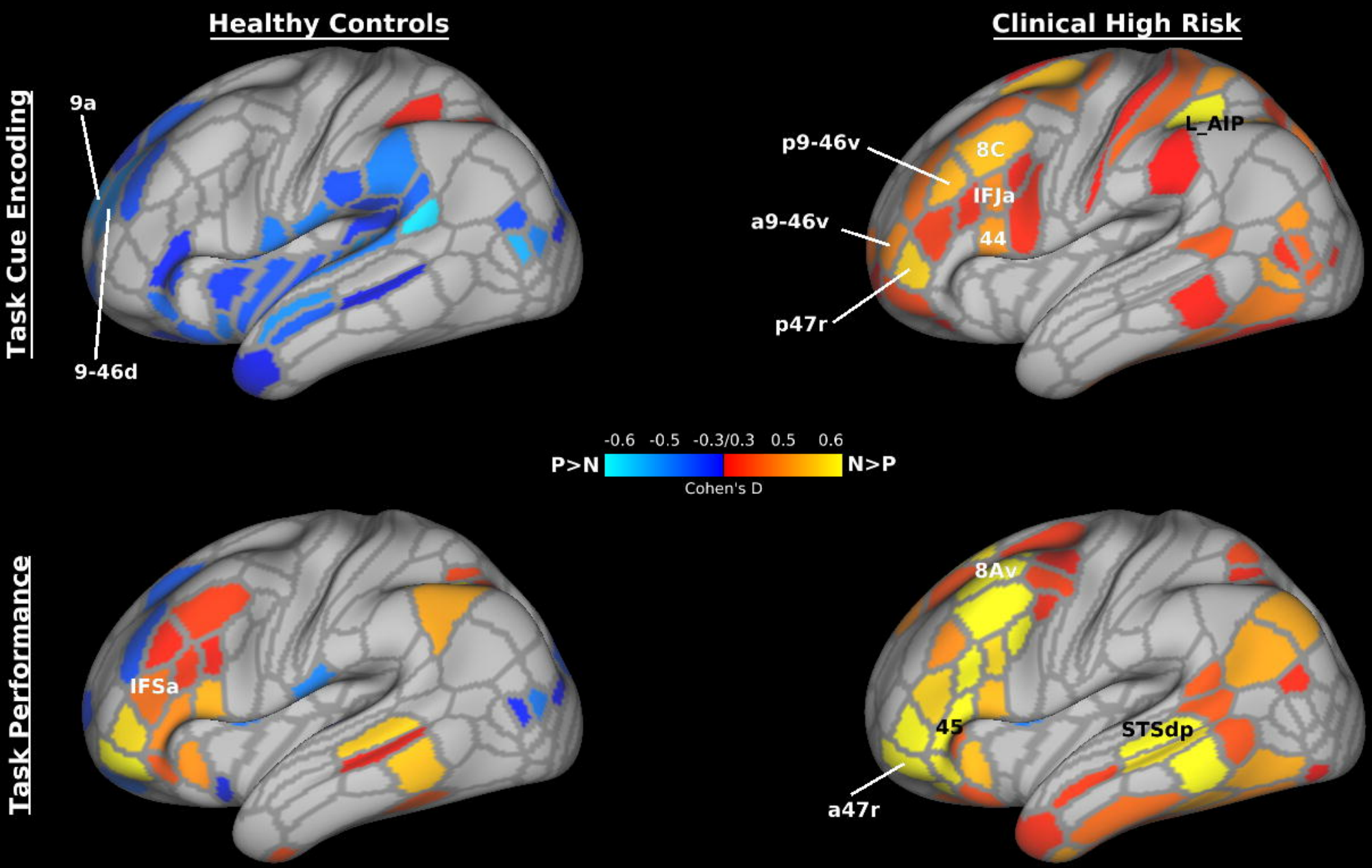

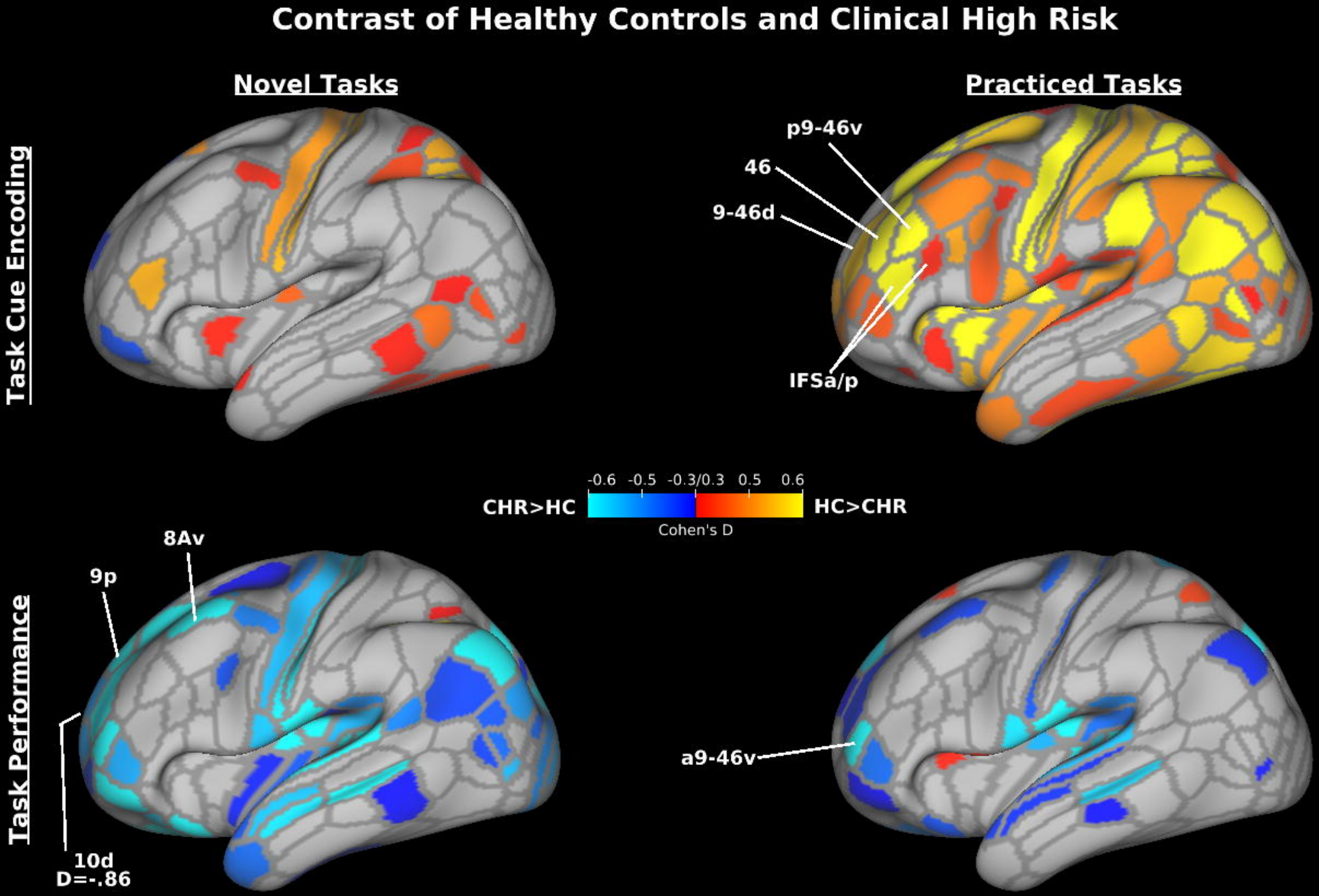
Contrast of Healthy Controls and Clinical High Risk
Novel Tasks
Practiced Tasks
Task Cue Encoding
Task Performance
p9-46v
46
9-46d
IFSa/p
-0.6 -0.5 -0.3/0.3 0.5 0.6
CHR>HC
HC>CHR
Cohen's D
8Av
9p
10d
D=-.86
a9-46v